Astronomy & Astrophysics manuscript no. 1504 October 14, 2004
(DOI: will be inserted by hand later)

Spectroscopic confirmation of high-redshift supernovae with the ESO VLT ⋆,⋆⋆

C. Lidman[1], D. A. Howell[2,3], G. Folatelli[4], G. Garavini[4,5], S. Nobili[4,5], G. Aldering[2], R. Amanullah[4], P. Antilogus[5], P. Astier[5], G. Blanc[2,6], M. S. Burns[7], A. Conley[2,8], S. E. Deustua[9], M. Doi[10], R. Ellis[11], S. Fabbro[12], V. Fadeyev[2], R. Gibbons[2], G. Goldhaber[2,8], A. Goobar[4], D. E. Groom[2], I. Hook[13], N. Kashikawa[14], A. G. Kim[2], R. A. Knop[15], B. C. Lee[2], J. Mendez[16,17], T. Morokuma[10], K. Motohara[10], P. E. Nugent[2], R. Pain[5], S. Perlmutter[2,8], V. Prasad[2], R. Quimby[2], J. Raux[5], N. Regnault[2,5], P. Ruiz-Lapuente[17], G. Sainton[5], B. E. Schaefer[18], K. Schahmaneche[5], E. Smith[15], A. L. Spadafora[2], V. Stanishev[4], N. A. Walton[19], L. Wang[2], W. M. Wood-Vasey[2,8], and N. Yasuda[20]

(The Supernova Cosmology Project)

1 European Southern Observatory, Alonso de Cordova 3107, Vitacura, Casilla 19001, Santiago 19, Chile
2 E. O. Lawrence Berkeley National Laboratory, 1 Cyclotron Rd., Berkeley, CA 94720, USA
3 Department of Astronomy and Astrophysics, University of Toronto, 60 St. George St., Toronto, Ontario M5S 3H8, Canada
4 Department of Physics, Stockholm University, Albanova University Center, S-106 91 Stockholm, Sweden
5 LPNHE, CNRS-IN2P3, University of Paris VI & VII, Paris, France
6 Osservatorio Astronomico di Padova, INAF, vicolo dell'Osservatorio 5, 35122 Padova, Italy
7 Colorado College, 14 East Cache La Poudre St., Colorado Springs, CO 80903
8 Department of Physics, University of California Berkeley, Berkeley, 94720-7300 CA, USA
9 American Astronomical Society, 2000 Florida Ave, NW, Suite 400, Washington, DC, 20009 USA.
10 Institute of Astronomy, School of Science, University of Tokyo, Mitaka, Tokyo, 181-0015, Japan
11 California Institute of Technology, E. California Blvd, Pasadena, CA 91125, USA
12 CENTRA-Centro M. de Astrofísica and Department of Physics, IST, Lisbon, Portugal
13 Department of Physics, University of Oxford, Nuclear & Astrophysics Laboratory, Keble Road, Oxford, OX1 3RH, UK
14 National Astronomical Observatory, Mitaka, Tokyo 181-0058, Japan
15 Department of Physics and Astronomy, Vanderbilt University, Nashville, TN 37240, USA
16 Isaac Newton Group, Apartado de Correos 321, 38780 Santa Cruz de La Palma, Islas Canarias, Spain
17 Department of Astronomy, University of Barcelona, Barcelona, Spain
18 Louisiana State University, Department of Physics and Astronomy, Baton Rouge, LA, 70803, USA
19 Institute of Astronomy, Madingley Road, Cambridge CB3 0HA, UK
20 Institute for Cosmic Ray Research, University of Tokyo, Kashiwa, 277 8582 Japan

Received June 22, 2004; accepted October 4, 2004

Abstract. We present VLT FORS1 and FORS2 spectra of 39 candidate high-redshift supernovae that were discovered as part of a cosmological study using Type Ia supernovae (SNe Ia) over a wide range of redshifts. From the spectra alone, 20 candidates are spectrally classified as SNe Ia with redshifts ranging from $z = 0.212$ to $z = 1.181$. Of the remaining 19 candidates, 1 might be a Type II supernova and 11 exhibit broad supernova-like spectral features and/or have supernova-like light curves. The candidates were discovered in 8 separate ground-based searches. In those searches in which SNe Ia at $z \sim 0.5$ were targeted, over 80% of the observed candidates were spectrally classified as SNe Ia. In those searches in which SNe Ia with $z > 1$ were targeted, 4 candidates with $z > 1$ were spectrally classified as SNe Ia and later followed with ground and space based observatories. We present the spectra of all candidates, including those that could not be spectrally classified as supernova.

Key words. supernovae:general – cosmology:observations

Send offprint requests to: C. Lidman: e-mail: `clidman@eso.org`

⋆ Based on observations obtained at the European Southern Observatory using the ESO Very Large Telescope on Cerro Paranal (ESO programs 265.A-5721(A), 67.A-0361(A), 267.A-5688(A), 169.A-0382(A) and (B)). Based in part on data collected at the Subaru Telescope, which is operated by the National Astronomical Observatory of Japan.

⋆⋆ Figures A.1 to A.39 are only available in electronic form via http://www.edpsciences.org.

1. Introduction

Over the past decade, observations of SNe Ia have played a leading role in measuring the expansion history of the Universe and in constraining cosmological parameters. It was through these observations that we discovered that the expansion is currently accelerating and that the Universe is presently dominated by an unknown form of dark energy with a negative equation of state (Perlmutter et al. 1998; Garnavich et al. 1998; Schmidt et al. 1998; Riess et al. 1998; Perlmutter et al. 1999; Tonry et al. 2003; Knop et al. 2003, Riess et al. 2004; Barris et al. 2004; for a review, see Perlmutter and Schmidt 2003).

When these results are combined with the results that have been derived from the fluctuations in the cosmic microwave background (Jaffe et al. 2001; Bennett et al. 2002; Spergel et al. 2003), the properties of massive clusters (Allen, Schmidt & Fabian 2002; Borgani et al. 2001) and the large scale structure of galaxies (Hawkins et al. 2003), a picture of a flat Universe dominated by dark energy emerges.

Considerable effort has been directed towards extending the redshift range over which SNe Ia are observed. The Hubble diagram of SNe Ia with $z \sim 0.5$ is degenerate to a linear combination of $\Omega_{\rm M}$ and Ω_{Λ}. Hence, an independent determination of these two parameters from SNe Ia at $z \sim 0.5$ is not possible. However, observations of SNe Ia over a wide range of redshifts and, in particular, very distant ($z \gtrsim 1$) SNe Ia can break this degeneracy (Goobar and Perlmutter 1995). With this aim in mind, and following a highly successful pilot search (Aldering 1998), the Supernova Cosmology Project (SCP) started a program to discover, spectrally confirm and photometrically monitor a substantial number of SNe Ia with redshifts beyond one.

In this paper, we present VLT FORS1 and FORS2 spectra of 39 candidate high redshift supernovae. We present all spectra, including those spectra for which a secure spectroscopic classification could not be made. The results of the photometric follow-up, the derived apparent magnitudes and the implications these measurements have for cosmology will be reported elsewhere.

2. Observations

2.1. Search and discovery

The candidates discussed in this paper were discovered during 8 separate, but not fully independent, high-redshift supernovae searches. The searches were divided into 4 observing campaigns that occurred during the Northern Springs of 2000, 2001 and 2002 and the Northern Fall of 2002. The observing campaigns, the months during which data were taken and the telescopes used in the searches are listed in Table 1.

Following the search and discovery techniques described in Perlmutter et al. (1995, 1997, 1999), the searches generally consisted of 2 to 3 nights of imaging to take reference images (images in which supernovae had not yet appeared), followed 3 to 4 weeks later by an additional 2 to 3 nights of imaging to take search images (images with the supernovae). In this paper, we refer to this type of search as a "standard" search, and searches 1,2, 3 and 5 were of this type. Searches 4, 6, 7 and 8, were a variation on this theme.

The Spring 2002 CFHT search (search 4 in Table 1), for example, was a "rolling" search, where images were taken once every few nights during a two week period. This was followed one, two and three months later by similar observations on the same fields. In this way, the search images of one month become the reference images of a later month, and, since images of the search fields are taken several times in any one month, one automatically gets a photometric time series without having to schedule follow-up observations separately, as one must do in a standard search.

The Subaru searches during the Spring and Fall of 2002 (searches 6, 7 and 8 in Table 1) also differed from the standard search. Searches 6 and 7 were "back-to-back" searches, in which the search images of the first search (search 6)became the reference images for the second search (search 7). Search 8 was a standard search that was then immediately followed with additional observations with the same instrument and telescope. This search offered the advantage of allowing us to follow several candidates simultaneously, rather than following candidates individually, as is the case with the standard search.

The data were processed to find objects that had brightened and the most promising candidates were given an internal SCP name and a priority. The priority is based on a number of factors: the significance of the detection, the percentage increase in the brightness, the distance from the center of the apparent host, the brightness of the candidate and the quality of the subtraction. The candidates were then distributed to teams working at the Gemini, Keck, Paranal, and Subaru Observatories for spectroscopic confirmation. The distribution was handled centrally and was done according to the priority of the candidates, the results from data that had been taken during previous nights, the capability and availability of the instruments and the telescopes at each of the observatories and the weather conditions at the individual observatories at any one time. Hence, the factors that affect whether or not a candidate is observed at any one observatory are complex and such factors would have to be taken into account in any statistical analysis. Note that these searches for extremely high-redshift supernovae are in this way more complex than previous searches that have been reported in our previous papers.

A preliminary analysis of the spectroscopic data is done within a day of when the data are taken - a more careful analysis is done later. Only those candidates that are confirmed as SNe Ia are then scheduled for follow-up observations, which consist of photometric monitoring in at least two broad-band filters during the first two months immediately following the discovery and final reference images, which are taken about one year later. These data are used to measure the peak magnitudes, the light curve widths, which are used to correct the peak magnitudes, and the colours of the SNe Ia. In some searches, such as searches 4 and 8 in Table 1, the optical follow-up is integrated into the search.

The aim of the spectroscopic follow-up is not to confirm as many SNe Ia as possible, but to provide a number of spectrally classified SNe Ia (typically four SNe Ia per campaign) to be scheduled for HST and ground-based follow-up within one to two days of the end of the spectroscopic runs. Without excep-

Table 1. The instruments and telescopes used during 4 campaigns. In general, a single campaign consisted of multiple searches. The prefix is used in the internal SCP candidate names. The individual searches are numbered for easy reference.

Campaign	Months	Instrument/Telescope	Search Number	Search type	Prefix
Spring 2000	April/May	CFHT12k/CFHT	1	Standard	C00
Spring 2001	March/April	CFHT12k/CFHT	2	Standard	S01
	March/April	MOSAICII/CTIO 4m Blanco	3	Standard	S01
Spring 2002	March to June	CFHT12k/CFHT	4	Rolling	C02
	April/May	MOSAICII/CTIO 4m Blanco	5	Standard	T02
	March/April	Suprime-Cam/Subaru	6[1]	Back-to-back	S02
	April/May	Suprime-Cam/Subaru	7[1]	Back-to-back	S02
Fall 2002	October/November	Suprime-Cam/Subaru	8[2]	Standard with additional wide-field monitoring	SuF02

[1] Searches 6 and 7 were part of the Subaru Deep Field Project (Kodaira et al. 2003).
[2] Search 8 was part of the Subaru XMM/Newton Deep Survey (Sekiguchi et al. in preparation)

tion, we succeeded in providing a sufficient number of SNe Ia for the follow-up.

We are presenting the spectra of all candidates that were observed with the ESO VLT, so there are a number of candidates that have only an internal SCP name. The SCP name consists of a prefix, which indicates at which telescope the candidate was discovered, and a running number. A list of prefixes is given in Table 1. The spectra of candidates that were not observed at the ESO VLT will be reported elsewhere.

2.2. Spectroscopic follow-up

The long slit spectroscopic modes of FORS1 and FORS2 (Appenzeller et al. 1998) on the ESO VLT were used to observe high priority candidates. For the purpose of long-slit spectroscopy, FORS1 and FORS2 are very similar instruments. The principle difference is that the detector in FORS1 is a single 2kx2k Tektronix CCD, while the detector in FORS2 is a mosaic of two 2kx4k red-optimized MIT CCDs. The FORS2 detector is more sensitive than the FORS1 detector, especially at red wavelengths. The availability of the red optimized CCDs in FORS2 after March 2002 made it possible to observe and confirm candidates at $z \sim 1.2$.

The dates during which the VLT spectroscopic observations took place and the redshift interval over which SNe Ia were targeted for VLT follow-up are listed in Table 2.

Three grisms (300V, 300I and 600z) and two slit widths (0.7 and 1.0 arc seconds) were used for the observations. In general, the grism was chosen to match the expected redshift of the candidate and the slit was matched to the seeing. The 300V grism was used with the GG435 order-sorting filter and the 300I and 600z grisms were used with the OG590 order-sorting filter.

Nearly all targets were acquired in the same way. The slit was placed through the candidate and a relatively bright and nearby pivot star. There were only three exceptions: SuF02-026 and SN 2002lc were observed together and SN 2000fr was acquired directly. The observational details are listed in Table 3. Generally speaking, three exposures with small offsets along the slit were taken for each candidate. Exceptions occurred when observations were aborted because we thought that we had sufficient data to identify the candidate or when we integrated longer for the fainter candidates.

Finding charts showing both the candidate and the pivot star are displayed in Fig. 1 and in Figs. A.1 to A.39. Candidates are marked with a cross and bright pivot stars are marked with either a box or a hexagon. Fainter pivot stars are circled and labelled alphabetically. The pivot star that was used during the acquisition is recorded in Table 3. In all finding charts, North is up and East is to the left.

In addition to the 39 candidates that were observed soon after they were discovered, the spectrum of the probable host galaxy of T02-047, which was observed several months after it was discovered, is also reported. The light curve of T02-047 indicates that it is a supernova.

3. Data reduction and classification

Standard IRAF[1] procedures were used to process the data. The bias was estimated by fitting the over-scan region with a low-order polynomial, flat-fielding was done with lamp flats that were first cleaned of parasitic light, and wavelength calibration was performed with arc frames.

For observations with the 300V grism, fringing is not a significant limitation in the data so the two-dimensional spectra were combined (with suitable clipping to remove cosmic rays) and the sky was removed by estimating the background flux on either side of the object trace.

For observations with the 300I and 600z grisms, fringing is more significant. If it is not treated carefully, the systematic error from fringing residuals can be large. Before combining individual spectra, a fringe correction was applied to the data. The fringe correction consists of the following steps:

[1] IRAF is distributed by the National Optical Astronomy Observatories, which are operated by the Association of Universities for Research in Astronomy, Inc., under the cooperative agreement with the National Science Foundation.

Table 2. Instruments and telescopes that were used in the spectroscopic follow-up.

Campaign	Instrument and Telescope	Dates	Observing Mode	Redshift Interval
Spring 2000	FORS1 on Antu (VLT-UT1)	12 May 2000	Service	$z = 0.3 - 0.7$
Spring 2001	FORS1 on Antu (VLT-UT1)	21-22 April 2001	Visitor	$z = 0.3 - 0.7$
		27 April and 28 May 2001	Service	$z = 0.3 - 0.7$
Spring 2002	FORS2 on Yepun (VLT-UT4) and	April-August 2002	Service	$z = 0.3 - 1.2$
	FORS1 on Melipal (VLT-UT3)	11-12 May 2002	Service	$z = 0.3 - 1.0$
Fall 2002	FORS2 on Yepun (VLT-UT4)	7-11 November 2002	Service	$z > 1$

Table 3. Summary of the observations. The SCP name is an internal name used by the SCP and is reported here as not all candidates have an IAU name.

SCP Name	IAU Name	Campaign	Coordinates of the candidate	Pivot Star	Offset	PA	MJD	Grism	Exp. (sec)
C00-008	SN 2000fr	Spring 00	13 42 00.14 +04 43 42.4	-[1]	-[1]	40.00	51676.2	300V	7200
S01-004	SN 2001gl	Spring 01	14 01 16.60 +05 12 48.9	Hex	-6.07, 0.16	92.41	52021.2	300V	3600
S01-005	SN 2001gm	Spring 01	14 01 51.18 +05 05 38.5	Hex	23.92, 24.80	43.97	52021.3	300V	2400
S01-007[4]	SN 2001go	Spring 01	14 02 00.95 +05 00 59.2	Hex	34.22, -4.46	97.42	52021.3	300V	2400
S01-007[4]	SN 2001go	Spring 01	14 02 00.95 +05 00 59.2	Hex	34.22, -4.46	97.43	52027.2	300V	7200
S01-007[4]	SN 2001go	Spring 01	14 02 00.95 +05 00 59.2	Hex	34.22, -4.46	97.43	52058.2	300V	9000
S01-017	SN 2001gr	Spring 01	10 04 23.27 +07 40 48.3	Box	-10.05,-24.64	22.19	52021.0	300V	3600
S01-028	SN 2001gs	Spring 01	10 00 52.68 +06 07 09.3	Box	11.89,-25.79	-24.75	52022.1	300V	4800
S01-031	SN 2001gu	Spring 01	10 03 28.61 +07 24 38.9	Hex	37.16, 3.32	84.89	52021.1	300V	4800
S01-033	SN 2001gw	Spring 01	15 43 45.86 +07 57 50.3	Hex	-14.09, 32.22	156.37	52021.4	300V	1200
S01-036	SN 2001gy	Spring 01	13 57 04.54 +04 30 59.8	Hex	21.49, 0.43	88.85	52021.3	300V	2400
S01-037	-	Spring 01	13 55 51.17 +04 48 06.7	Hex	-56.87, 32.41	119.68	52021.1	300V	3600
S01-054	SN 2001ha	Spring 01	10 06 33.50 +07 38 03.2	Hex	13.51, 22.72	30.74	52022.0	300V	3600
S01-065	SN 2001hc	Spring 01	09 44 31.52 +08 02 02.8	Hex	-14.17, 46.46	-16.96	52022.1	300V	1800
S02-000	SN 2002fd	Spring 02	14 03 54.08 +04 59 49.0	Box	-6.48, 2.62	112.01	52376.1	300V	600
S02-001	-	Spring 02	14 03 56.42 +05 23 16.6	Hex	-27.85, 39.10	144.54	52376.3	300I	2700
S02-002	SN 2002fe	Spring 02	14 04 18.16 +05 19 25.6	B	-8.49, 1.52	100.15	52376.2	300I	2700
S02-025	-	Spring 02	13 57 50.11 +05 17 25.5	Hex	0.09, 14.94	0.34	52376.2	300I	2700
S02-075	SN 2002fg	Spring 02	13 24 25.92 +27 44 33.9	Hex	57.74,-22.44	-68.76	52431.0	300V	7200
C02-016	SN 2002fr	Spring 02	14 00 46.40 +04 33 41.4	Hex	-12.67 10.57	145.65	52400.3	300V	900
C02-028	SN 2002fm	Spring 02	14 00 29.75 +04 46 50.1	B	-27.76, 21.91	128.28	52413.0	300V	1800
C02-030	SN 2002fp	Spring 02	14 02 18.40 +04 47 05.9	Hex	1.69,-21.86	-4.43	52407.1	300I	3600
C02-031	-	Spring 02	14 01 38.07 +04 38 02.2	Box	0.88, 38.36	178.69	52406.1	300I	3600
C02-034	-	Spring 02	14 00 30.75 +05 13 55.6	Hex	5.82,-22.77	-14.34	52413.0	300V	1800
T02-015	SN 2002gi	Spring 02	13 57 12.25 +04 33 16.8	Hex	1.17,-68.78	-0.97	52407.2	300I	7200
T02-028	SN 2002gj	Spring 02	15 36 25.48 +09 28 18.2	Hex	-40.55, 62.58	147.06	52413.2	300V	3000
T02-029	SN 2002gk	Spring 02	15 37 07.47 +09 36 18.7	C	-20.24, 16.98	129.99	52413.3	300V	900
T02-030	SN 2002gl	Spring 02	15 43 24.40 +07 53 57.5	Hex	2.32, 43.98	-176.98	52413.1	300V	3000
T02-047[3]	-	Spring 02	15 36 29.88 +09 38 42.8	Hex	-42.94,-29.25	55.74	52494.0	300V	3000
SuF02-002	SN 2002kq	Fall 02	02 17 12.24 -04 55 08.7	Hex	-21.25, -4.06	79.18	52586.1	300I	3600
SuF02-005	-	Fall 02	02 18 35.67 -04 31 11.2	A	18.26, 0.06	-90.19	52586.1	300I	3600
SuF02-007	-	Fall 02	02 18 52.32 -05 01 14.0	Hex	6.63,-40.66	-9.26	52588.7	300I	13200
SuF02-012	SN 2002lc	Fall 02	02 18 51.60 -04 47 25.7	Hex[2]	-19.04, 14.75	8.81	52588.3	600z	7200
SuF02-017	SN 2002kn	Fall 02	02 16 45.71 -05 09 51.2	Hex	-48.24, -0.53	89.37	52590.2	300I	1800
SuF02-025	SN 2002km	Fall 02	02 16 23.93 -04 49 29.4	Box	-7.30, 5.14	125.15	52588.1	300I	3600
SuF02-026	-	Fall 02	02 18 51.90 -04 46 57.4	Hex[2]	-19.04, 14.75	8.81	52588.3	600z	7200
SuF02-028	SN 2002kz	Fall 02	02 16 56.36 -05 00 58.1	Hex	26.08,-47.36	-28.84	52587.1	300I	3600
SuF02-051	-	Fall 02	02 17 27.47 -04 40 45.3	C	-11.62, -2.10	79.76	52586.3	300I	3600
SuF02-060	SN 2002kr	Fall 02	02 17 34.51 -04 53 46.6	A	19.82,-17.49	-48.75	52587.2	300I	3600
SuF02-065	SN 2002ks	Fall 02	02 17 34.53 -05 00 15.4	A	-28.15,-23.05	50.69	52586.2	300I	3600
SuF02-081	-	Fall 02	02 20 07.49 -05 08 27.4	A	51.24,-20.89	-67.82	52589.2	300I	9600
SuF02-083	SN 2002kx	Fall 02	02 18 06.21 -05 00 38.8	Box	-35.39, 1.64	92.65	52587.1	300I	7200

[1] Centered on the candidate.
[2] The slit passed through SuF02-012 and SuF02-026
[3] T02-047 was observed several months after maximum light
[4] SN 2001go was observed at three epochs

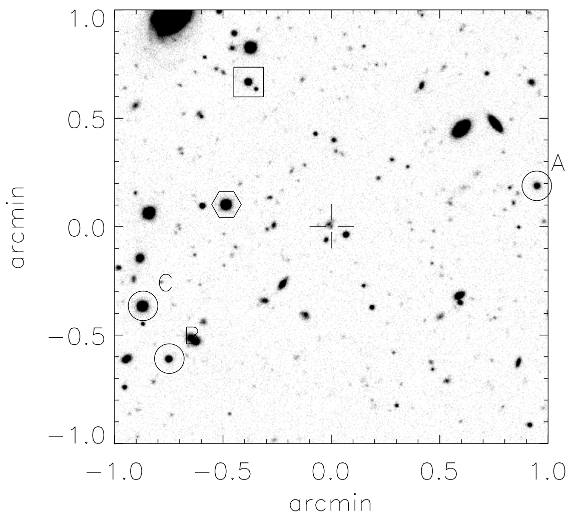

Fig. 1. A finding chart centered on SN 2000fr (C00-008). North is up and East is to the left. The candidate is marked with a cross and bright pivot stars are marked with either a box or a hexagon. Fainter pivot stars are circled and labelled alphabetically. The pivot star that was used during the acquisition is recorded in Table 3. The finding charts of other candidates are available in the appendix.

- For a given spectrum in which the object was at a certain slit position, a group of similar spectra (the same grism, order sorting filter and slit) with objects at different slit positions was collected.
- Fringe frames are created by clipping object pixels and averaging the remainder. Since the intensity of night sky lines can vary with respect to one another, each column (the spatial direction of the spectra are along columns) is treated individually. Instrumental flexure for FORS1 and FORS2 is small, so some fringe frames were created from data that were taken on different nights.
- The fringe frames are subtracted from the data after suitable scaling. Again, each column is treated individually.
- An average sky spectrum (calculated by averaging along columns of the fringe frame) is added back to the data. This helps with the clipping of cosmic rays when the two dimensional spectra are combined.
- The data are combined with suitable clipping for cosmic rays and the sky is removed by estimating the flux on either side of the object trace.

The resulting two-dimensional sky-subtracted spectra are free of fringes at the expense of a slight reduction in the statistical signal-to-noise ratio.

The spectra of the candidates and, in some cases, the spectra of the hosts were then extracted and calibrated in wavelength and flux. In all cases, we also produce error spectra, which are used to estimate the significance of spectral features.

The signal-to-noise ratio varies from very low ($\lesssim$ 1 per wavelength element) to moderately good ($\gtrsim$ 10 per wavelength element). The spectra with the highest signal-to-noise ratios are studied in more detail in Garavini et al. (in preparation). The quality of some of the high-redshift SN Ia spectra that are presented in this paper, SN 2002ks at z=1.181 is one example (see Fig. A.37), matches the quality of spectra that have been taken with HST (Riess et al. 2004).

3.1. Classification

At high redshifts ($z \gtrsim 0.4$), the broad Si II feature at 6150 Å, which is one of the defining spectral signatures of the SN Ia class, is often outside the wavelength range covered by the spectra. Therefore, we use other features, such as the Si II feature at ~ 4000 Å and the S II "W" feature at ~ 5400 Å, which are only seen in SNe Ia, to spectrally identify SNe Ia when the Si II feature at ~ 6150 Å is not visible (Hook et al. in preparation).

We also use a library of galaxy and nearby supernova spectra to fit the spectra of candidates (Howell and Wang, 2002), and we use these fits to classify candidates when the Si II and S II features cannot be clearly identified. A representative sample of galaxy spectral templates ranging from early to late types and more than 250 spectra of nearby supernova of all types currently make up the library. For a given candidate and a given nearby supernova, the fit determines the fraction of host galaxy light, the host galaxy spectral type, the redshift of the supernova and the amount of reddening. The quality of the fit is quantified with the reduced χ^2, which has little meaning in an absolute sense. The finite size of the spectral library and systematic calibration errors in both low and high samples mean that the reduced χ^2 is always greater than one. However, it is useful for ordering the fits.

The fit can be constrained by using additional information. For example, if there is no apparent host - SN 2001ha is one example - the fraction of light from the host galaxy is set to zero in the fit. Alternatively, if there is a host and if the redshift of the host galaxy is known, the redshift of the candidate is fixed to this value and the redshift is reported to three decimal places. Otherwise, the redshift is determined from the fit and is reported to two decimal places.

The fits are ordered according to the reduced χ^2 and the first dozen fits are inspected visually. If Silicon or Sulfur are clearly identified or if the spectrum can be matched with the spectrum of a nearby SN Ia, the candidate is assigned the label "Ia" and the classification is considered secure. Less secure candidates are labelled "Ia*". The asterisk indicates some degree of uncertainty. This usually means that we see spectral features that are consistent with a SN Ia classification and can find an acceptable match with a nearby SN Ia, but that other types, such as a SN Ic, also result in acceptable matches and cannot be excluded. For example, the spectra of SNe Ia 10 days after maximum light resemble the spectra of some SNe Ic at maximum light, especially around the 4000 Å region. In these cases, the light curve can be used to estimate the epoch at which the spectra were taken and to distinguish between the two possibilities. A good example is the spectrum of SN 2002gj, which can be matched with either a SN Ia or a SN Ic. By using the light curve to constrain the epoch, SN 2002gj is clearly a SN Ia.

The best matching nearby supernova is chosen by visually examining the best dozen fits and selecting the best qualitative fit. For candidates that are classified as "Ia" or "Ia*", the best matches are listed in Table 4 and plotted in Fig. 3 and in Figs. A.1 to A.39.

A simple dash indicates that a classification based on the VLT spectrum alone could not be made. This does not mean that these candidates are not supernovae. Some of the unclassified candidates show broad supernova-like features in their spectra, while others have well measured light curves. Candidates that fall in the former category include SN 2001gl, SN 2002lc and SuF02-007. Candidates that fall in the latter category include SN 2002fr, SN 2002fm, C02-034, T02-047, SN 2002kq, SuF02-007, SN 2002lc, SuF02-026, SN 2002kz, SuF02-051 and SN 2002kx.

4. Results

The results of the four SCP campaigns are summarized in Table 4, where each candidate is identified with the internal SCP name. The IAU name, the spectral classification, the redshift and the best template match are also listed if these items are available. Beside each classification, we also give the reason for the classification. If Si II at 4000 Å or 6150 Å or S II at 5400 Å were identified then we attach the label "Si II" to the classification. If the classification was done from the fit, we attach the label "SF", which stands for spectral fit. The comments provide additional information. For example, in the cases where a classification from the VLT spectrum could not be made, we note down any relevant information from the light curve.

The spectrum of SN 2000fr is shown in Fig. 3 and the spectra of all other candidates are presented in the appendix[2]. In some cases, we have compensated for telluric absorption by dividing the spectra with a suitably scaled spectrum of the telluric absorption on Cerro Paranal. In any case, the location of telluric absorption features (usually the A and B bands and, for the 300I and 600z grisms, the telluric feature that starts at 9300 Å) are marked in all spectra with the symbol ⊕. The location of night sky subtraction residuals (usually from the bright night sky lines at 5577, 5890, 6300 and 6364 Å) are marked with the letters "NS". Spectroscopic features from the host galaxy are marked where appropriate.

In the comparison plots, nearby SNe are shown in blue, while the observations minus the host galaxy template are shown in black. In most cases, the observations have been rebinned to 20 Å.

The results[3] are summarized as follows:

– 39 candidates were observed.
– 20 candidates are classified as SNe Ia.
– 1 candidate is classified as a possible Type II supernova.
– Of the remaining 18 unclassified candidates, labelled with a dash in Table 4, 11 have broad supernova-like spectral features and/or have supernova-like light curves. One of these 11 candidates - SuF02-026 - has two strong emission lines that cannot be identified.
– Of the remaining 7 candidates, 5 have neither clear supernova features nor sufficient photometric follow-up to measure a light curve, but posses a galaxy component from which a redshift can be determined.
– The remaining 2 candidates have featureless continua.

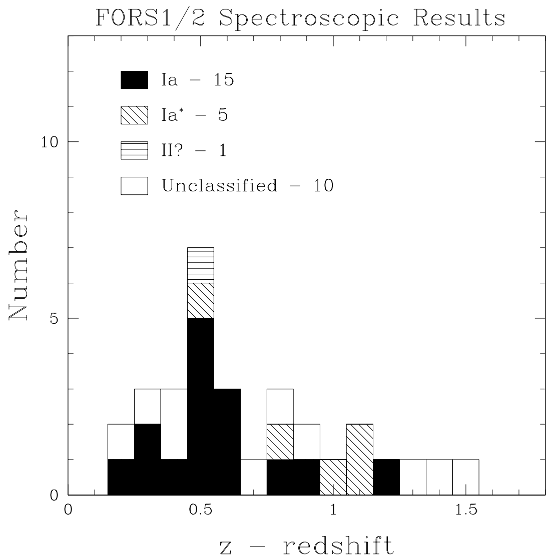

Fig. 2. A redshift histogram of the candidates.

A redshift histogram is shown in Fig. 2. Of the eight candidates that do not have redshifts, three have broad spectral features and two have supernova-like light curves.

5. Discussion

In terms of classifying candidates from the spectra alone, there is a clear correlation between the number of candidates that are classified as SNe Ia and the redshift at which SNe Ia were targeted. In searches 1, 2, 3 and 5, (See Table. 1), where SNe Ia at $z \sim 0.5$ were targeted for VLT spectroscopic follow-up, 13 out of 16 candidates (excluding T02-049) are classified as SNe Ia. In search 8, where SNe Ia with $z > 1$ were targeted for VLT spectroscopic follow-up, 4 out of 13 candidates are classified as SNe Ia.

There are multiple reasons for the large difference. The aim of search 8 was to find several $z > 1$ SN Ia and the strategy of the spectroscopic follow-up was tuned to make the best use of the time that was available. In general, each candidate was first observed for one hour. Candidates that were found to have $z < 1$ were no longer observed. This included SuF02-002, SuF02-005, SN 2002km and SuF02-028. In one case (SN 2002km) a secure classification could be made. In the other three cases, a supernova might have been identified if we had chosen to integrate longer. Alternatively, if the can-

[2] The appendix is only available in the electronic version of the journal.
[3] T02-047 is not considered since the spectrum was taken many months after it was discovered.

Table 4. Classifications, redshifts and nearby supernova matches. Redshifts based on the host are quoted to an accuracy of three decimal places. Redshifts based on the fit are quoted to two. The comments provide additional information on each candidate.

SCP Name	IAU Name	Spectroscopic Classification		Redshift	Template Match	Comments
C00-008	SN 2000fr	Ia	Si II	0.543	SN 1990N -7 days	
S01-004[2]	SN 2001gl	-	-	-	-	Broad spectral features and no detectable host.[3]
S01-005[2]	SN 2001gm	Ia	Si II	0.478	SN 1992A +5 days	
S01-007[2]	SN 2001go	Ia	Si II	0.552	SN 1992A +5 days	
S01-017	SN 2001gr	Ia	SF	0.540	SN 1996X +2 days	
S01-028	SN 2001gs	-	-	0.658		Host dominated.
S01-031	SN 2001gu	Ia	SF	0.777	SN 1999bp +1 day	
S01-033	SN 2001gw	Ia	Si II	0.363	SN 1989B -1 day	
S01-036	SN 2001gy	Ia	Si II	0.511	SN 1990N -7 days	
S01-037	-	-	-	-		Featureless blue spectra.
S01-054	SN 2001ha	Ia	Si II	0.58	SN 1981B Max.	No detectable host.[3]
S01-065	SN 2001hc	Ia	Si II	0.35	SN 1981B Max.	Faint host.
S02-000	SN 2002fd	Ia	Si II	0.279	SN 1990N -7days	
S02-001	-	-	-	1.424		
S02-002	SN 2002fe	Ia*	SF	1.086	SN 1999ee -8 days	
S02-025	-	-	-	-		Featureless
S02-075	SN 2002fg	Ia*	SF	0.78	SN 1999bm +6 days	
C02-016	SN 2002fr	-	-	0.303?		Blue spectrum. Supernova-like light curve.
C02-028	SN 2002fm	-	-	0.448		Host dominated. Supernova-like light curve. Small percentage increase.
C02-030	SN 2002fp	-	-	0.352		
C02-031	-	II?	SF	0.541	SN 1999em Max.	Host dominated. Small percentage increase.
C02-034	-	-	-	0.243		Host dominated. Small percentage increase.
T02-015	SN 2002gi	Ia	Si II	0.912	SN 1996X +2 days	
T02-028	SN 2002gj	Ia*	SF	0.45	SN 1992A +9 days	Small percentage increase.
T02-029	SN 2002gk	Ia	Si II	0.212	SN 1992A +6 days	
T02-030	SN 2002gl	Ia	Si II	0.510	SN 1989B -5 days	
T02-047[1]	-	-	-	0.489		Supernova-like light curve.
SuF02-002	SN 2002kq	-	-	0.823		Supernova-like light curve.
SuF02-005	-	-	-	0.863		Small percentage increase.
SuF02-007	-	-	-	1.16?	SN 1981B Max.	No host.[3] Broad spectral features and supernova-like light curve.
SuF02-012	SN 2002lc	-	-	1.3?	SN 1999aa -3 days	Broad spectral features. Supernova-like light curve.
SuF02-017	SN 2002kn	Ia*	SF	1.03	SN 1999bm +3 days	Faint host. Supernova-like light curve.
SuF02-025	SN 2002km	Ia	Si II	0.606	SN 1990N -7 days	
SuF02-026	-	-	-	-		Two unidentified lines. Supernova-like light curve.
SuF02-028	SN 2002kz	-	-	0.347		Host dominated. Supernova-like light curve.
SuF02-051	-	-	-	-		Featureless. No detectable host[3] and supernova-like light curve.
SuF02-060	SN 2002kr	Ia*	SF	1.063	SN 1981B Max.	Host dominated. Small percentage increase. Supernova-like light curve.
SuF02-065	SN 2002ks	Ia	Si II	1.181	SN 1981B Max.	
SuF02-081	-	-	-	1.478		Narrow light curve
SuF02-083	SN 2002kx	-	-	1.272		Small percentage increase. Supernova-like light curve.

[1] T02-047 was observed several months after maximum light

[2] These candidates were discovered at the CFHT. The remainder of the candidates with the prefix "S01" were discovered at CTIO.

[3] This refers to the reference images. On deeper images, a host might become visible.

didate showed evidence for broad features or if the redshift from host galaxy lines (in particular [OII]) placed the host at $z > 1$, the candidates were re-observed during later nights. As the amount of allocated time was limited, not all promising candidates could be followed. These factors led to a lower overall yield at $z < 1$, but they also enabled us to confirm several $z > 1$ SNe Ia and to obtain their redshifts.

Nevertheless, the spectroscopic confirmation of $z > 1$ SNe Ia is challenging. At $z \sim 1$, SNe Ia are about 1.5 magnitudes fainter than at $z \sim 0.5$. Additionally, the spectral features that one uses for classification shift further and further into the red

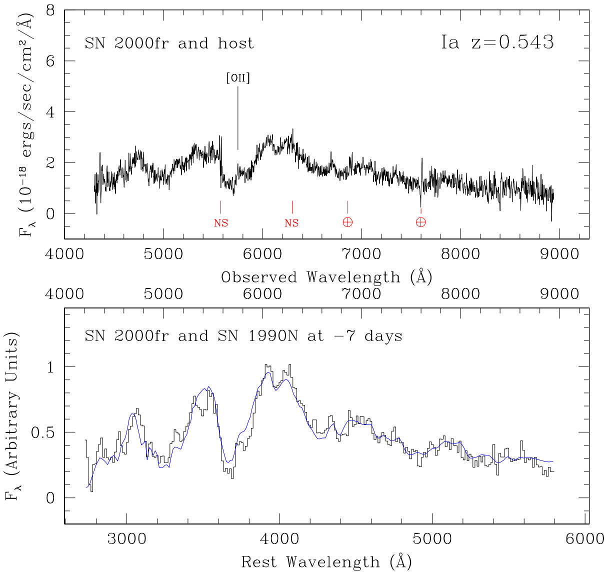

Fig. 3. A spectrum of SN 2000fr, a SN Ia at $z = 0.543$ with unambiguous detection of Si II at 4000 Å. In the upper spectrum, the unbinned spectrum of the candidate is plotted in the observer's frame and is uncorrected for host galaxy light. Night sky subtraction residuals are marked with the letters "NS" and telluric absorption features are marked with the symbol ⊕. In the lower spectrum, contamination from the host is removed and the spectrum is rescaled and rebinned by 20 Å. This spectrum is plotted in black and it is plotted in both the rest frame (lower axis) and the observer's frame (upper axis). For comparison, the best fitting nearby supernova is plotted in blue. SN 2000fr was first identified as a SN Ia in a very early spectrum that was taken with LRIS on the KeckII telescope on 2001 May 4th and was subsequently observed again with FORS1. The FORS1 spectrum has one of the highest S/N ratios of all securely identified supernovae in this paper. SN 2000fr was followed in the J-band with ISAAC 2004 and in the R- and I-bands with HST and ground-based telescopes (Knop et al. 2003). The J-band observations, which corresponds to the rest-frame I-band, show a clear second maximum about 30 days after the first maximum. A spectrum of the host galaxy (not shown here) shows emission in [OII] and [OIII] as well as Balmer absorption lines.

where sky subtraction can be difficult because of variable night-sky emission and detector fringing. This can be partially compensated by integrating longer and using instruments and telescopes that are efficient in the 600 to 1000 nm spectral region. Although the spectra of SNe Ia show significant features shortward of the broad CaII feature at 3900 Å that could be used to aid the classification, the lack of good quality UV spectra for nearby supernovae of all types means that these features cannot be used without using features that are further into the red.

For $z > 1$, which have peak magnitudes near I $\sim$ 25, an additional source of ambiguity appears. Given the typical signal-to-noise that one can achieve with state-of-the-art instrumentation, one can sometimes match the spectra equally well with SNe Ia at two different redshifts. Fortunately, host galaxy lines, either [OII] or H and K or sometimes all three, can be used to measure a precise redshift in most cases. In this paper, SNe 2002fe, 2002gi, 2002kn, 2002kr and 2002ks fall into this category. However, in other cases, such as SuF02-007 and SN 2002lc, there are no clear galaxy lines, even though the spectra of these candidates show broad features.

In terms of classifying candidates from the spectra alone, there is also a correspondence between the selection criteria that are used to select candidates and the percentage of candidates that are spectrally identified as SNe Ia. In the rolling search with the CFHT, none of the 5 candidates could be spectrally confirmed as a SN Ia. For comparison, in the Spring 2002 search with CTIO, all four candidates (excluding T02-049) were confirmed as SNe Ia. Although the numbers are small, they are significant. The search area and candidate selection criteria of the rolling search were such that the search was also sensitive to relatively fainter supernovae (Type II or SN 1991bg-like supernovae) on relatively brighter hosts. The spectra confirm this as many of the candidates from the rolling search are dominated by the light of the host galaxy.

The contribution from the host galaxy can be approximately quantified with the percentage increase in the flux of the candidate between the search and reference images. A small increase usually means a significant amount of host contamination. A very large or formally infinite increase usually means little or no host contamination. The flux is measured over a fixed aperture whose diameter depends on the seeing. The signal-to-noise ratio of the detection over the same fixed aperture provides a measure of the significance of the detection. A low signal-to-noise ratio usually means that the candidate is faint, and this could mean that the candidate, if it is a SN Ia, is either very distant or has been caught very early. In Fig. 4 the signal-to-noise ratio of the detection is plotted against the percentage increase for candidates that were brighter than I = 24.7 at the time of discovery.[4] Candidates from the CFHT 2002 search are highlighted with large circles. The figure shows that classification from spectroscopy is generally not successful if the percentage increase is below $\sim$ 25%. The boundary of this region is marked with a dashed line in Fig. 4. Candidates in which the percentage increase is less than 25% are thus noted in Table 4.

Not one of the candidates has broad emission lines that would indicate that it is an AGN. This demonstrates that our selection strategy, which selects against candidates having small intensity variations that are also precisely centered on the host galaxy, is quite effective in rejecting AGNs.

In this paper, we have strictly used only the spectra for classification purposes and all the classifications listed in Table 4 are based on the spectra alone. However, in searches like the CFHT Spring 2002 search and the Subaru Fall 2002 search, where spectroscopic confirmation is difficult because the candidates are near relatively bright hosts or because the candidates are relatively faint, additional information such as the light curve or the colour of the candidate can become part of the criteria used for classification. The strategy of these two searches was such that most of the candidates were also monitored during the subsequent weeks and months. Of the 18 candidates that were observed in these two surveys, 5 were spec-

[4] For the surveys done in R-band, we use R = 24.7

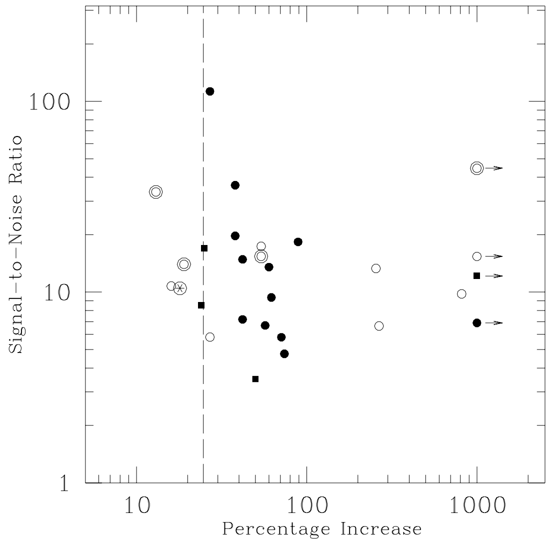

Fig. 4. The percentage increase versus the signal-to-noise ratio for candidates that were brighter than I = 24.7 at the time of discovery. Candidates that were classified as Ia (Ia*) are plotted with solid circles (squares), C02-031 - a possible SN II - is plotted as a star and unclassified candidates are plotted with open circles. Candidates from the CFHT 2002 search are highlighted with large circles. Candidates with arrows have percentage increases that are greater than 1000%, which means that the host was considerably fainter than the candidate and perhaps undetected. The dashed line marks the region where the percentage increase is 25% or less. Candidates in this region are difficult to classify spectrally.

trally classified as either Ia, Ia* or II?. Of the remaining 13 candidates, 10 were followed with sufficient coverage (more than 4 light curve points) and 9 have supernova-like light curves. This includes SN 2002fr, SN 2002fm, SN 2002kq, SuF02-007, SN 2002lr, SuF02-026, SN 2002kz, SuF02-051 and SN 2002kx. These cases are noted in Table 4 and in the comments on individual candidates.

6. Summary

We have presented VLT FORS1 and FORS2 spectra of 39 candidate high-redshift supernovae that were discovered as part of a program to discover SNe Ia over a wide range of redshifts. By comparing these spectra with the spectra of nearby SNe Ia, 20 candidates have been identified as SNe Ia with redshifts ranging from $z = 0.212$ to $z = 1.181$.

Of the remaining 19 candidates that cannot be spectrally identified as SNe Ia, one candidate might be a Type II supernova at $z = 0.541$ and 11 candidates exhibit broad supernova-like spectral features and/or have supernova-like light curves. Of the final 7 candidates that cannot be confirmed as supernova, (either from the light curves or the spectra), 5 possess a galaxy component, from which redshifts ranging from $z = 0.347$ to $z = 1.478$ have been been measured, and 2 show featureless blue continua.

Acknowledgements. This work would not have been possible without the dedicated efforts of the daytime and nighttime support staff at the Cerro Paranal Observatory. We thank ECT* (European Centre for Theoretical Studies in Nuclear Physics and Related Areas) for the support they provided during the preparation of this paper. The Subaru searches were supported in part with a scientific research grant (15204012) from the Ministry of Education, Science, Culture, and Sports of Japan, and in part by the Japanese Society for the Promotion of Science (a Bilateral Research Program between Japan and USA). The CFHT is operated by the National Research Council of Canada, the Centre National de la Recherche Scientifique of France and the University of Hawaii. The authors would like to thank the CFHT queue team for the efficient operation of the CFHT12k camera. This work was supported in part by the Director, Office of Science, Office of High Energy and Nuclear Physics, of the U.S. Department of Energy under Contract No. DE-AC03-76SF00098. Support for this work was provided by NASA through grants HST-GO-08346.01-A , HST-GO-08585.14-A , HST-GO-09075.01-A , from the Space Telescope Science Institute, which is operated by the Association of Universities for Research in Astronomy, Inc., under NASA contract NAS 5-26555.

References

Aldering, G. 1998, IAUC 7046
Allen, A. W., Schmidt, R. W., & Fabian, A. C. 2002, MNRAS, 334, L11
Appenzeller, I., Fricke, K., Fürtig, W., et al. 1998, The Messenger, 94, 1
Barris, B. J., Tonry, J. L., Blondin, S., .et al. 2004, ApJ, 602, 571
Bennett, C. L., Halpen, M., Hinshaw, G., et al. 2003, ApJS, 148, 1
Borgani, S., Rosati, P., Tozzi, P., et al. 2001, ApJ, 561, 13
Garnavich, P. M., Kirshner, R. P., Challis, P., et al. 1998, ApJ, 493, L53
Goobar, A. & Perlmutter, S. 1995, ApJ, 450, 14
Hawkins, E., Maddox, S., Cole, S., et al. 2003, MNRAS, 346, 78
Howell, D. A. & Wang, L. 2002, AAS, 201, 9103.
Jaffe, A. H.. Ade, P., Balbi, A., et al. 2001, Phys. Rev. Lett., 86, 3475
Kniazev, A. Y., Pustilnik, S. A. Grebel, E., et al. 2004, ApJS, 153, 429
Kodaira,K. Taniguchi,Y. Kashikawa,N. et al. 2003, PASJ, 55L, 17
Knop, R. A., Aldering, G. A., Amanalluh, R., et al. 2003, ApJ, 598, 102
Perlmutter, S., Pennypacker, C. R., Goldhaber, G., et al. 1995, ApJ, 440, L41
Perlmutter, S., Gabi, S., Goldhaber, G., et al. 1997, ApJ, 483, 565
Perlmutter, S., Aldering, G., della Valle, M., et al. 1998, Nature, 391, 51
Perlmutter, S., Aldering, G., Goldhaber, G. et al. 1999, ApJ, 517, 565
Perlmutter, S. and Schmidt, B. 2003, in "Supernovae & Gamma Ray Bursts", ed. Weller, K. (Springer)
Riess, A. G., Filippenko, A. V., Challis, P. et al. 1998, AJ, 116, 1009
Riess, A. G., Strolger, L.-G., Tonry, J. et al. 2004, ApJ, 607, 665.
Nobili, S. 2004, Ph. D. thesis, Stockholm Univ.
Schmidt, B. P., Suntzeff, N. B., Phillips, M. M., et al. 1998, ApJ, 507, 46
Spergel, D. N., Verde, L., Peiris, H. V. et al. 2003, ApJS, 148, 175
Stern, D. et al. 2000, ApJ, 537, 73
Tonry, J. L., Schmidt, B. P., Barris, B., et al. 2003, ApJ, 594, 1

Online Material

Appendix A: Finding charts, spectra and notes on individual candidates

This section contains finding charts and spectra of all candidates except SN 2000fr, which are shown in Figs. 1 and 3. The candidates are labelled with either their IAU names or their internal SCP names if no IAU name was assigned.

In the finding charts, North is up and East is to the left. The candidate is marked with a cross and bright pivot stars are marked with either a box or a hexagon. Fainter pivot stars are circled and labelled alphabetically. The pivot star that was used during the acquisition is recorded in Table 3. The finding charts were created from the images that were taken during the reference and search runs. Regions that appear blank are regions that are outside the field of view.

In general, the spectrum of the candidate is plotted twice. In the upper spectrum, the unbinned spectrum of the candidate is plotted in the observer's frame and is uncorrected for host galaxy light. Night sky subtraction residuals are marked with the letters "NS" and telluric absorption features are marked with the symbol ⊕. In the lower spectrum, the spectrum is rescaled, contamination from the host (if any) is removed, an extinction correction is applied and the spectrum is re-binned, typically by 20 Å. This spectrum is plotted in black and it is plotted in both the rest frame (lower axis) and the observer's frame (upper axis). For comparison, the best fitting nearby supernova is plotted in blue. The extinction correction can correct for extinction either in the host or the comparison spectrum. If the candidate could not be classified, only the upper spectrum is plotted.

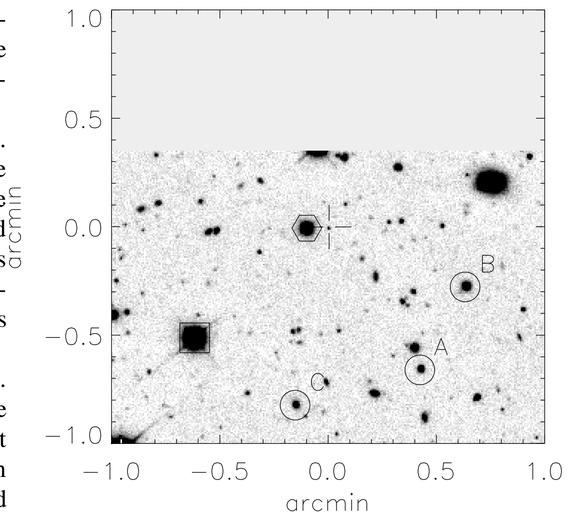

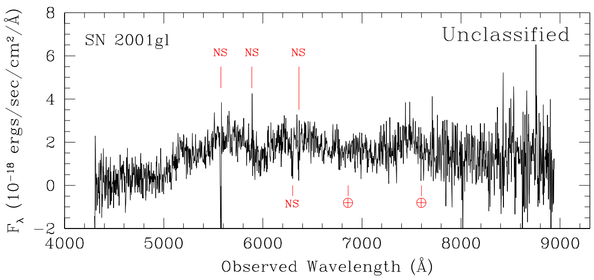

Fig. A.1. Above, a finding chart centered on SN 2001gl (S01-004), an unclassified candidate at an unknown redshift, and below, the spectrum. This unusual candidate has very broad spectral features; however, it was not possible to match this candidate with any of the supernovae in our nearby catalog. No host was detectable in the reference image, and the search images, which were taken 16 and 20 days after the reference image, indicate that the candidate was real and stationary, implying that it was not a solar system body. The spectrum was taken 21 days after the reference images.

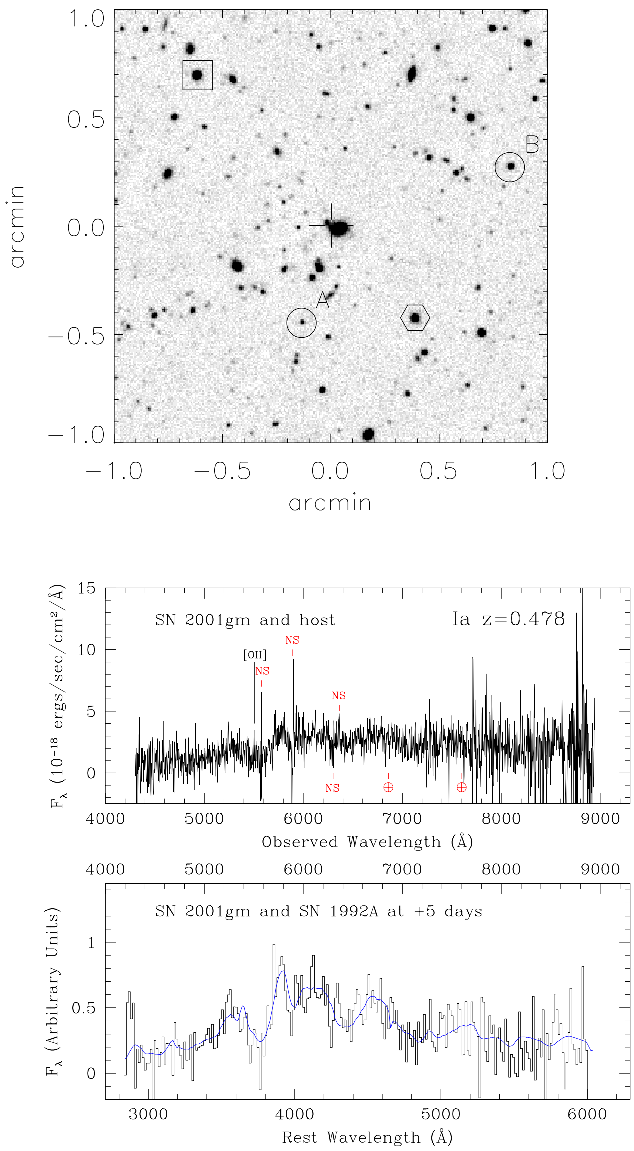

Fig. A.2. Above, a finding chart centered on SN 2001gm (S01-005), a SN Ia at z = 0.478 and below, the spectrum. Although a bright night sky line contaminates the 4000 Å region, the Si II feature at 4000 Å is clearly detected. A separate spectrum of the host (not shown here) shows weak [OII] emission.

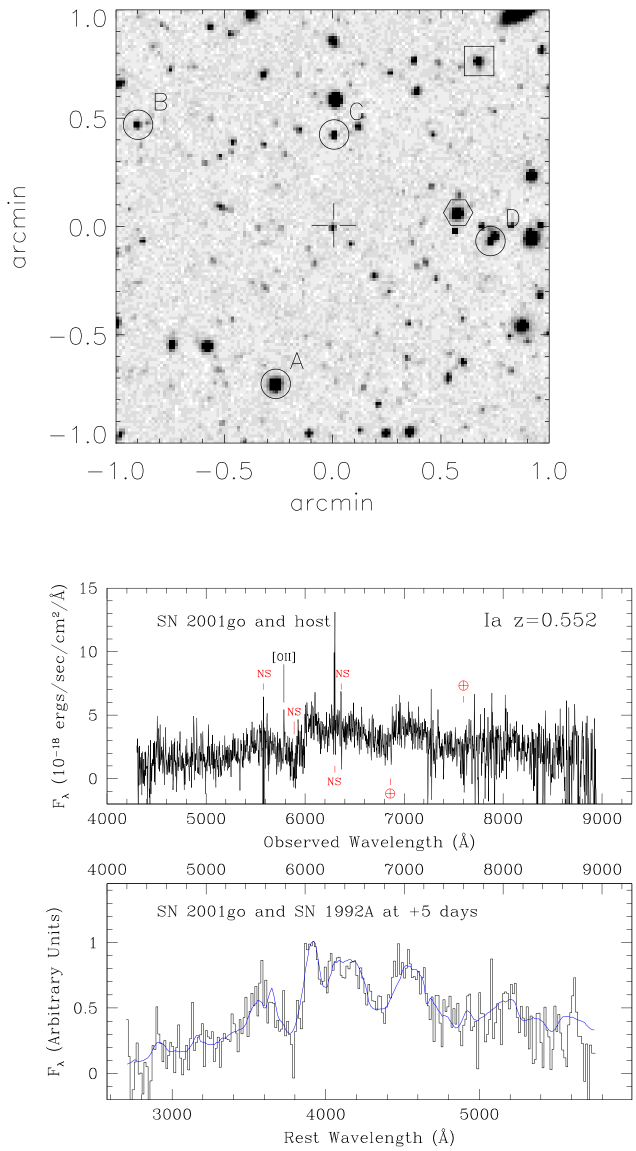

Fig. A.3. Above, a finding chart centered on SN 2001go (S01-007), a SN Ia at z = 0.552, and below, the spectrum. This candidate was observed at three epochs. The initial confirmation spectrum (shown here) was taken on 2001 May 21. The Si II feature at 4000 Å feature can be clearly seen. Additional deeper spectra (not shown here) were taken 6 and 37 observer-frame days later (Garavini et al. in preparation).

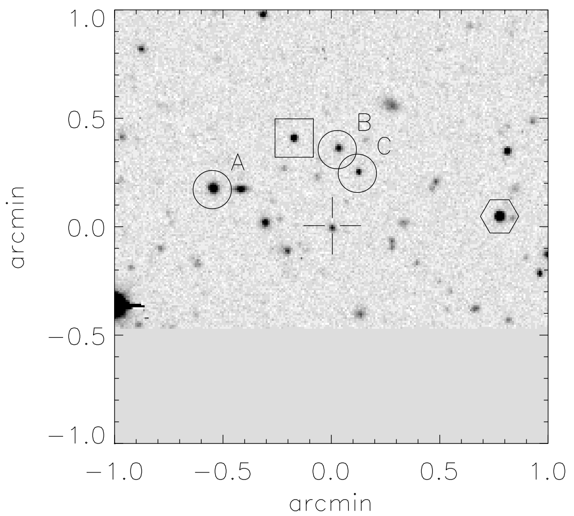

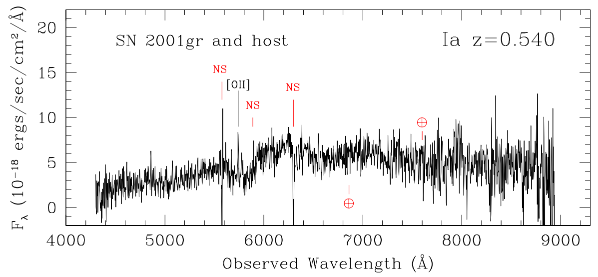

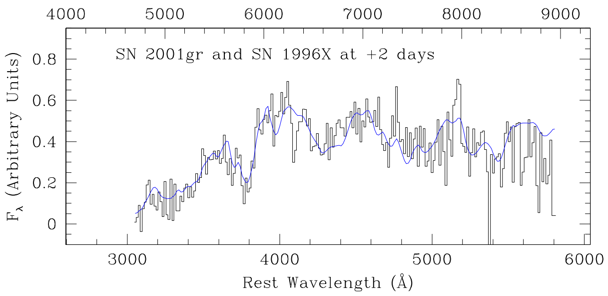

Fig. A.4. Above, a finding chart centered on SN 2001gr (S01-017), a SN Ia at z = 0.540, and below, the spectrum. Although Si II feature at 4000 Å is not clearly detected in this candidate, the data are significantly better fit with SN Ia spectra than with the spectra of other types.

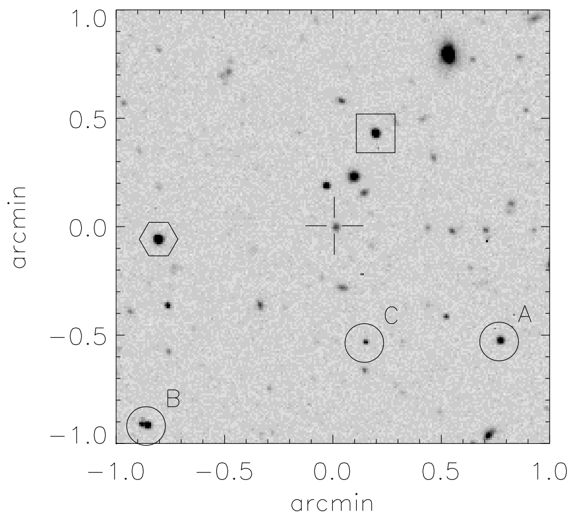

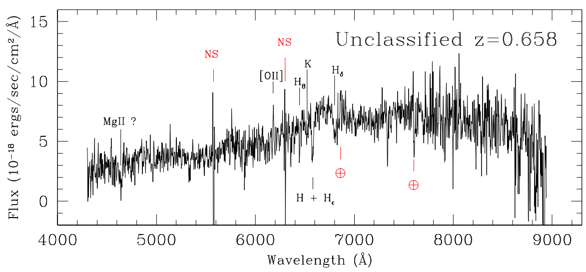

Fig. A.5. Above, a finding chart centered on SN 2001gs (S01-028), an unclassified candidate at z = 0.658, and below, the spectrum. This is a faint candidate on a bright host that was observed during a period of relatively poor seeing. The percentage increase in the flux was only 27%, so most of the light in the spectrum is from the host, which has several Balmer absorption lines.

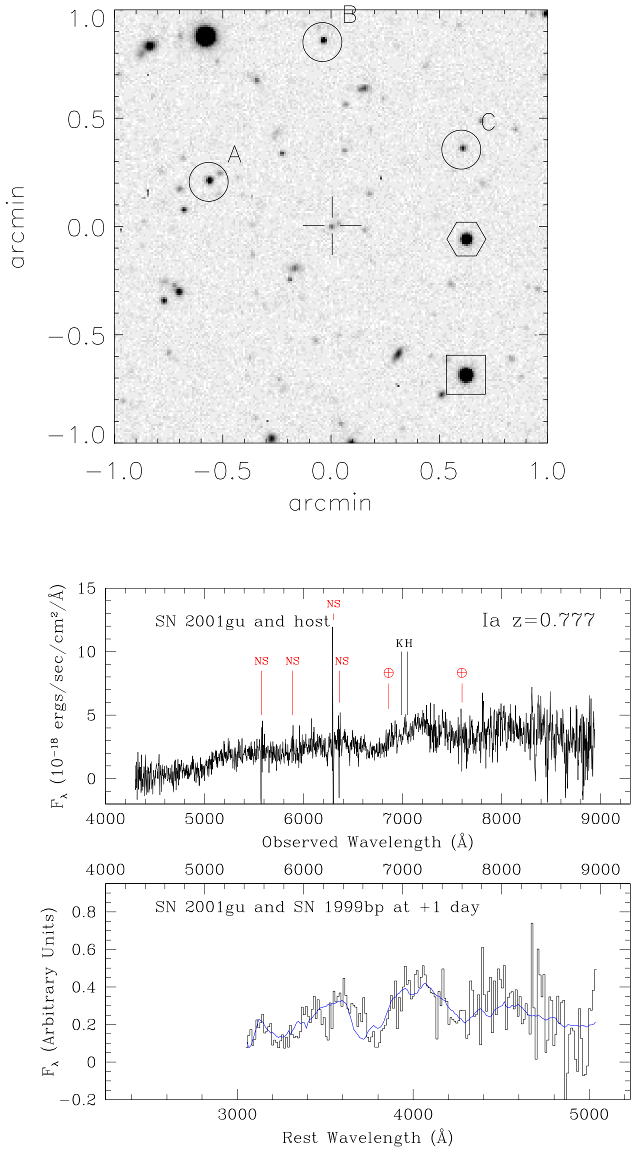

Fig. A.6. Above, a finding chart centered on SN 2001gu (S01-031), a SN Ia at z = 0.777, and below, the spectrum. The host shows CaII H and K absorption lines and no detectable [OII] emission which suggests an early-type host. Since the Si II feature at 4000 Å is weak and contaminated by the H and K lines of the host, the classification is based on the fit. The redshift of the fit was constrained to that of the host. The wavelength coverage of the best matching nearby SN Ia, SN 1999bp, is restricted to rest frame wavelengths that are greater than 3000 Å, so the comparison is limited to these wavelengths.

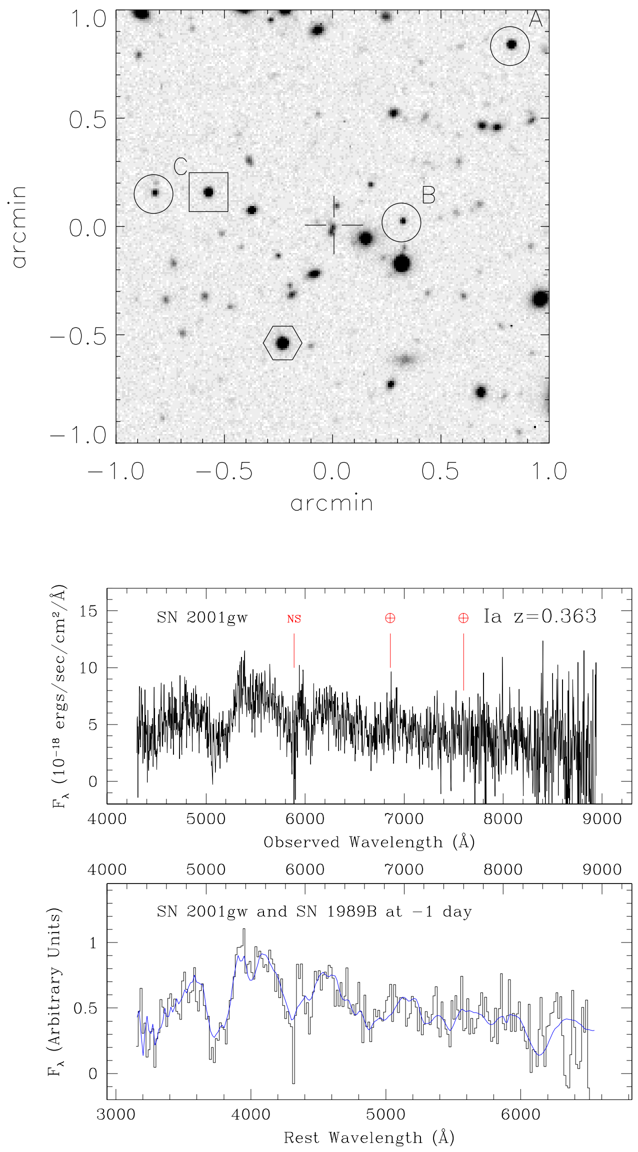

Fig. A.7. Above, a finding chart centered on SN 2001gw (S01-033), a SN Ia at z = 0.363, and below, the spectrum. In addition to the Si II feature at 4000 Å, the Si II at 6150 Å is also visible. The redshift is derived from an [OII] emission line in the spectrum of the host galaxy (not shown here).

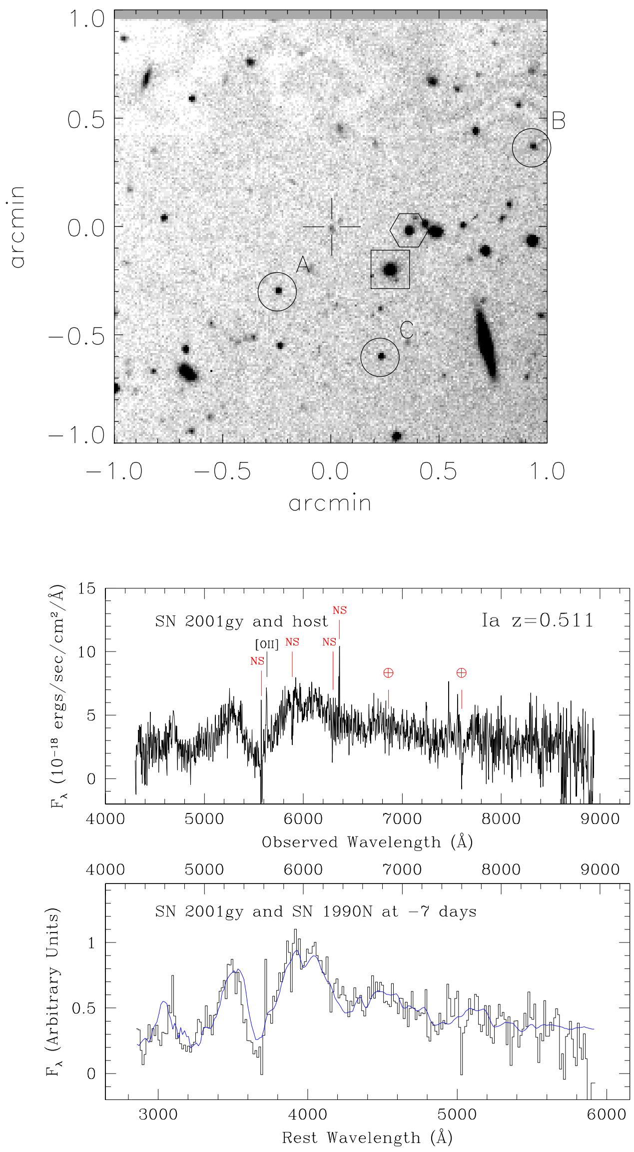

Fig. A.8. Above, a finding chart centered on SN 2001gy (S01-036), a SN Ia at $z = 0.511$, and below, the spectrum. The Si II feature at 4000 Å is clearly detected.

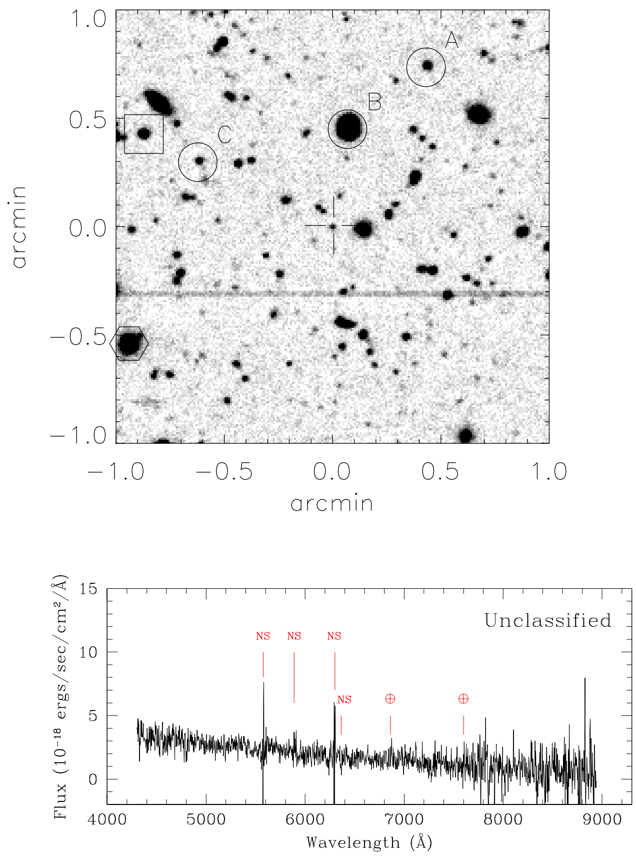

Fig. A.9. Above, a finding chart centered on S01-037, and below, the spectrum. Neither the classification nor the redshift of this candidate is known. The spectrum shows a strong blue continuum which is characteristic of Type II supernovae before maximum light; however, with neither a redshift nor clear spectral features, a classification cannot be made. The candidate was detected on search images that were taken on different dates and is stationary, so it is not an asteroid nor an artifact.

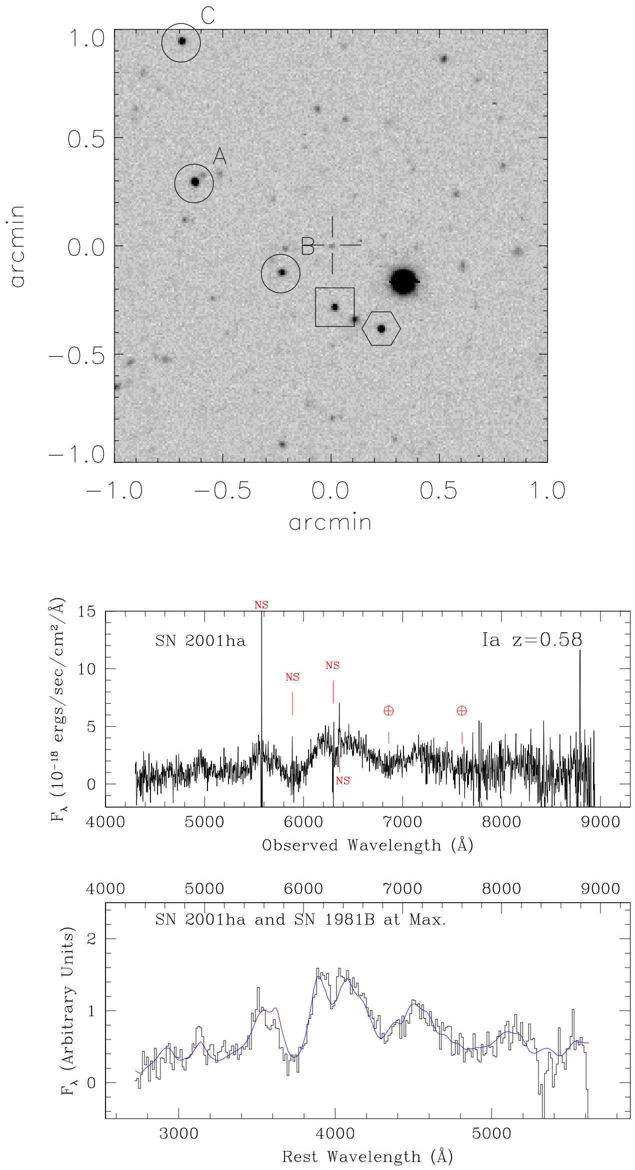

Fig. A.10. Above, a finding chart centered on SN 2001ha (S01-054), a SN Ia at $z = 0.58$, and below, the spectrum. There are no spectral features from the host and a host is not visible in the reference image, so the redshift is determined from the fit. The Si II feature at 4000 Å is clearly detected.

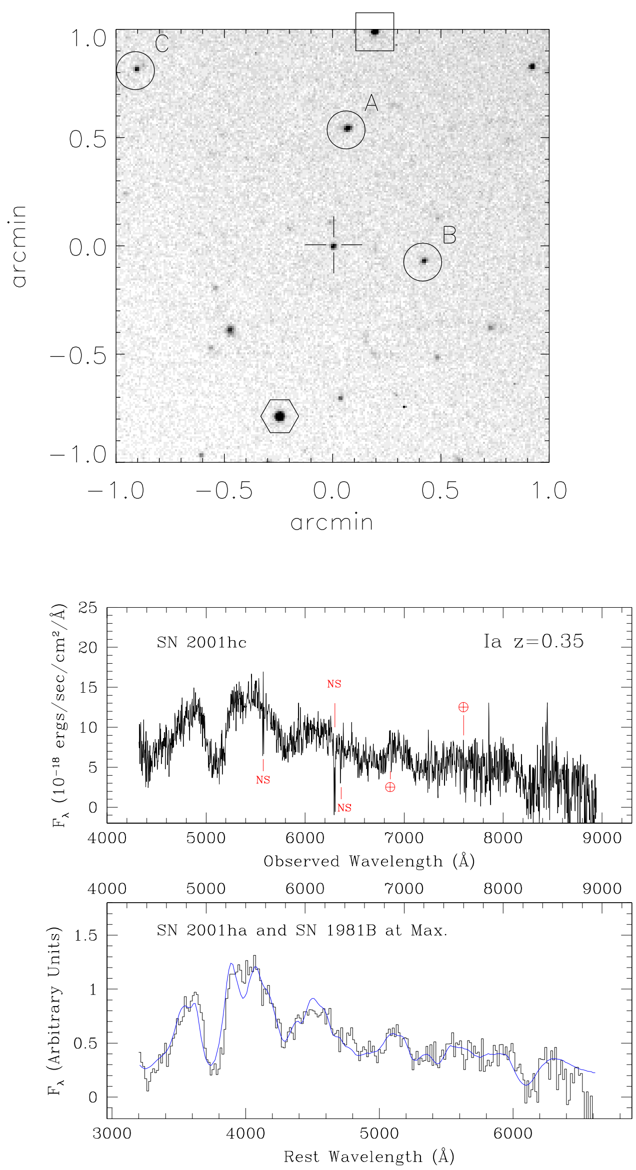

Fig. A.11. Above, a finding chart centered on SN 2001hc (S01-065), a SN Ia at $z = 0.35$, and below, the spectrum. This relatively nearby candidate has Si II at 6150 Å, S II at 5400 Å, and Si II at 4000 Å. There are no spectral features from the host, so the redshift is determined from the fit. In the reference image, a very faint host is visible.

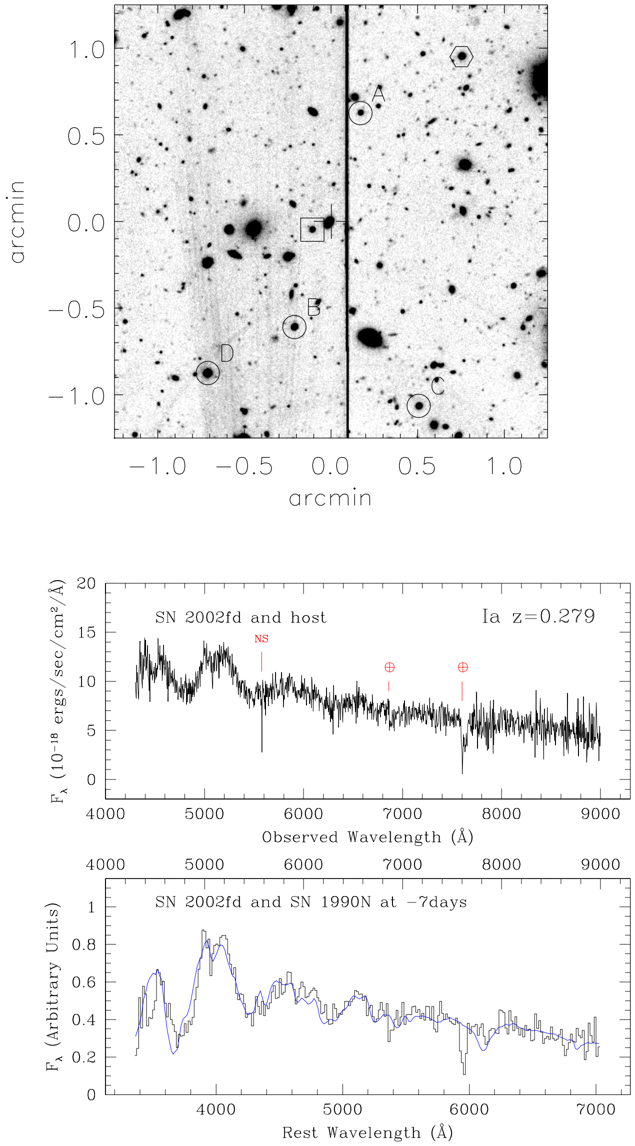

Fig. A.12. Above, a finding chart centered on SN 2002fd (S02-000), a SN Ia at z = 0.279, and below, the spectrum. The Si II feature at 4000 Å is clearly detected, but the Si II feature at 6150 Å is relatively weak.

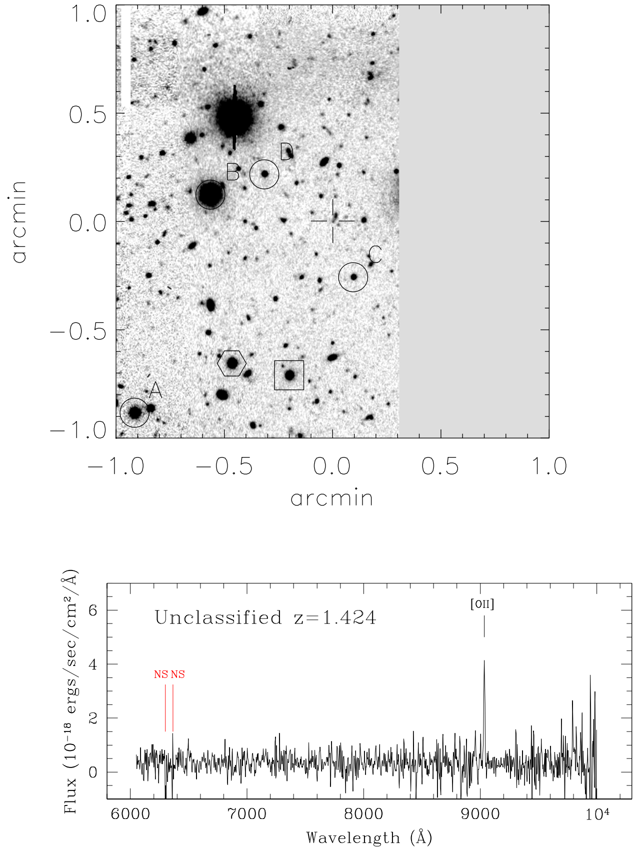

Fig. A.13. Above, a finding chart centered on S02-001, an unclassified candidate at z = 1.424, and below, the spectrum. A single strong line and a featureless continuum. Given the width and shape of the line and the lack of other lines in the wavelength range covered by the spectra, the line is identified as the [OII] doublet at 3727 Å. It is unlikely that the line is Lyα at $z > 5$ because the characteristic asymmetry of Lyα in galaxies at $z > 5$ (Stern et al. 2000) and the jump in the continuum across the line are not evident in these spectra. Nor is the line likely to be Hα, as neither Hβ nor [OIII] are detected. The equivalent width of the line is greater than 50 Å so the host galaxy would be classified as an emission line galaxy (ELG) if the line were Hα (Kniazev et al. 2004). In ELGs, Hβ is typically three times weaker than Hβ and the strengths of [OIII] and Hα are roughly equivalent. Given the strength of the detected line in these spectra, both [OIII] and Hβ should have been detected if the line was Hα.

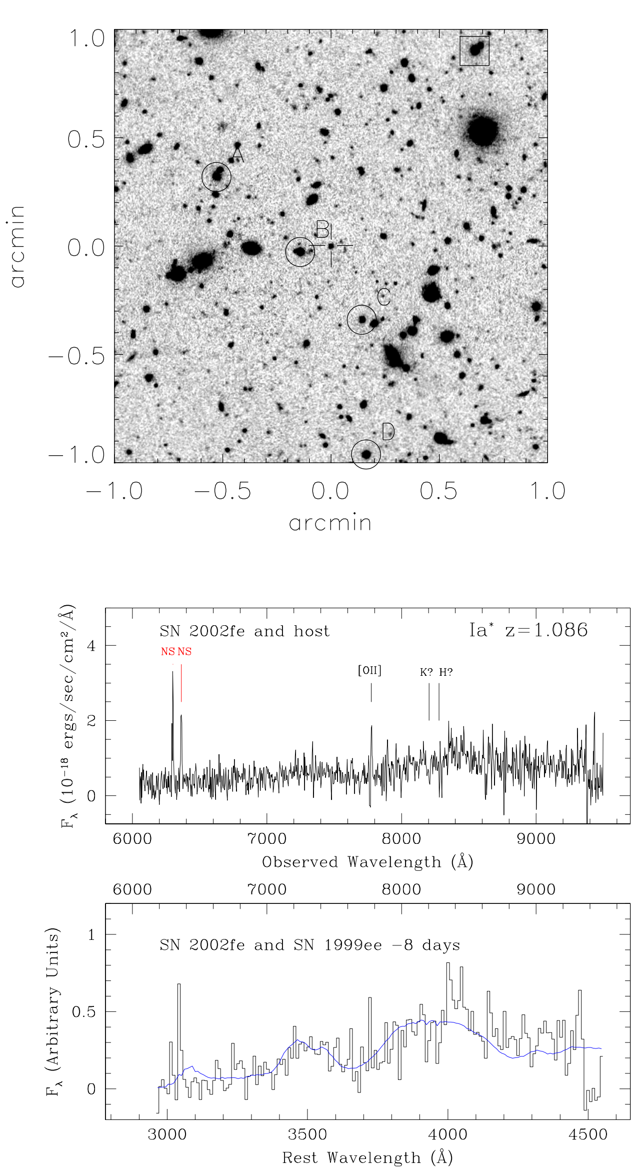

Fig. A.14. Above, a finding chart centered on SN 2002fe (S02-002), a SN Ia* at $z = 1.086$, and below, the spectrum. The profile of the line that we have identified as [OII] is affected by a nearby bright night sky line; however, the line is clearly detected in the 2-dimensional spectrum. This line, together with the probable detection of the H and K Ca II lines in the host, enables us to measure a secure redshift. The signal-to-noise ratio of the spectrum is relatively low and the Si II feature at 4000 Å is not detected, so the the classification is qualified with an asterisk. In some nearby SNe Ia that are observed one to two weeks before maximum light, the Si II feature is absent. The best fit nearby SN Ia, SN 1999ee, shows no Si II at 4000 Å.

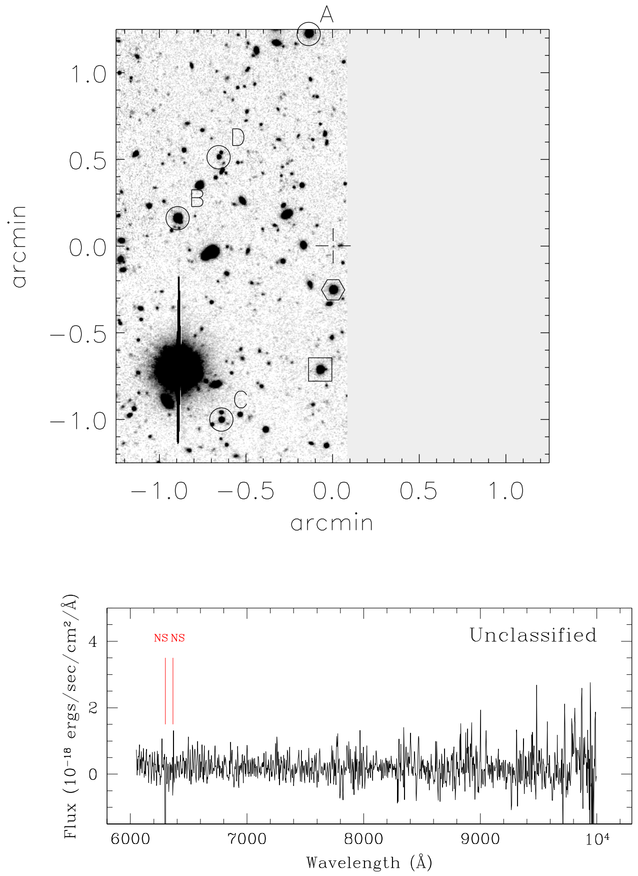

Fig. A.15. Above, a finding chart centered on S02-025 and below, the spectrum. This candidate has a blue continuum with no significant spectral features. It has neither a classification nor a redshift.

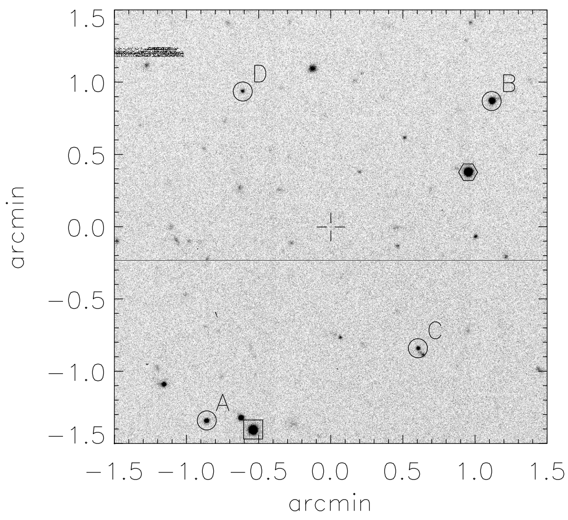

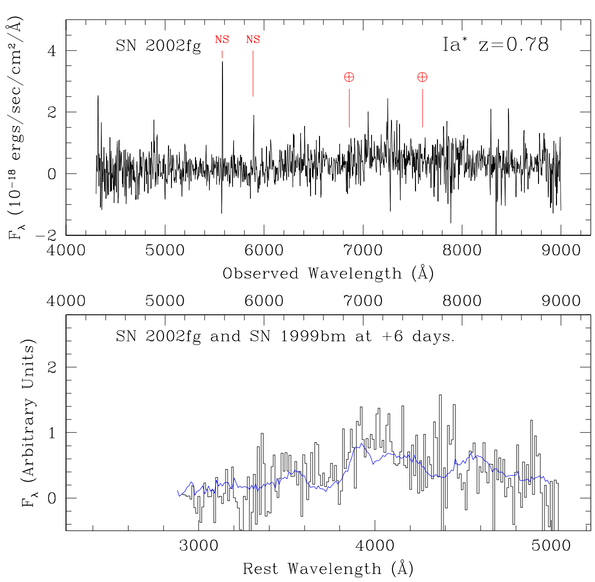

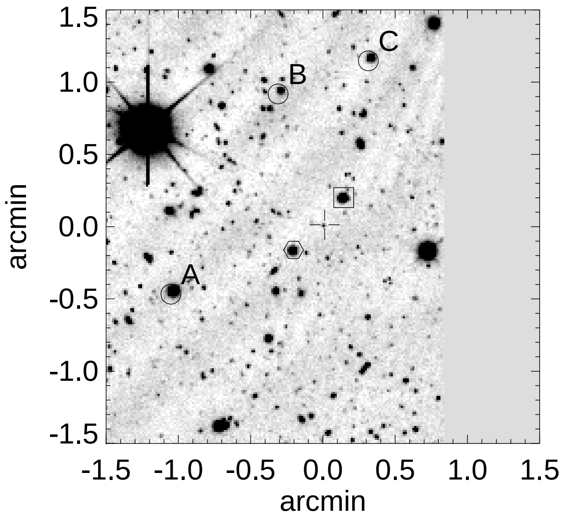

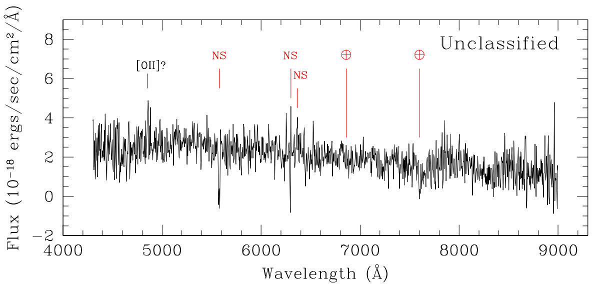

Fig. A.17. Above, a finding chart centered on SN 2002fr (C02-016), an unclassified candidate that might be at $z = 0.303$, and below, the spectrum. This candidate has a very well sampled light curve (7 points), which shows a dramatic rise over the first 5 days. The spectrum is dominated by slightly irregular blue continuum and there is a very weak line which would put the host at $z = 0.303$ if the line is identified as [OII].

Fig. A.16. Above, a finding chart centered on SN 2002fg (S02-075), a SN Ia* at $z = 0.78$, and below, the spectrum. Since the Si II feature at 4000 Å is not clearly detected in this candidate and since there are no spectral features from the host, the classification and the redshift are derived from the fit. The candidate was observed several weeks after it was discovered, so it is likely that the spectrum was taken past maximum light. The best matching nearby SN Ia is SN 1999bm at 6 days past maximum light. The signal-to-noise ratio is also relatively low and the SiII feature at 4000 Å is not detected, so the classification is qualified with an asterisk.

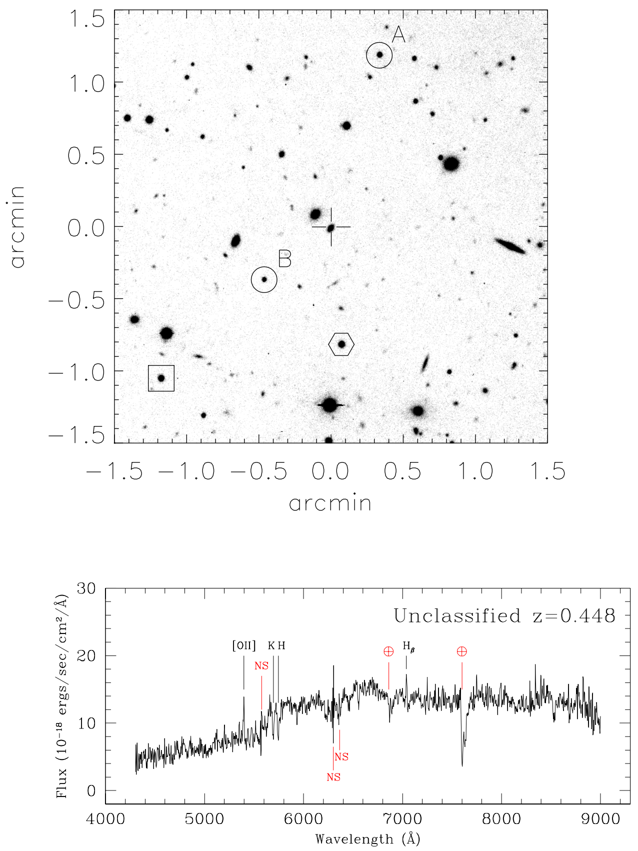

Fig. A.18. Above, a finding chart centered on SN 2002fm (C02-028), an unclassified candidate at $z = 0.448$, and below, the spectrum. The percentage increase in this candidate was very small, only 13%, and the spectrum is dominated by the light from the host galaxy. However, there is excess flux at 6600 Å and 5600 Å that might be from a supernova. Unfortunately, an acceptable fit with a nearby SN Ia was not possible. In such cases, the fit depends critically on how well the galaxy template matches the spectrum of the host galaxy. Relatively small errors can leave significant residuals which can make the matching difficult. The most secure way of fitting this candidate will be take a spectrum of the host after the supernova has faded. The candidate is offset from the center of the host and the light curve is well sampled with four points before maximum light and four points after maximum light.

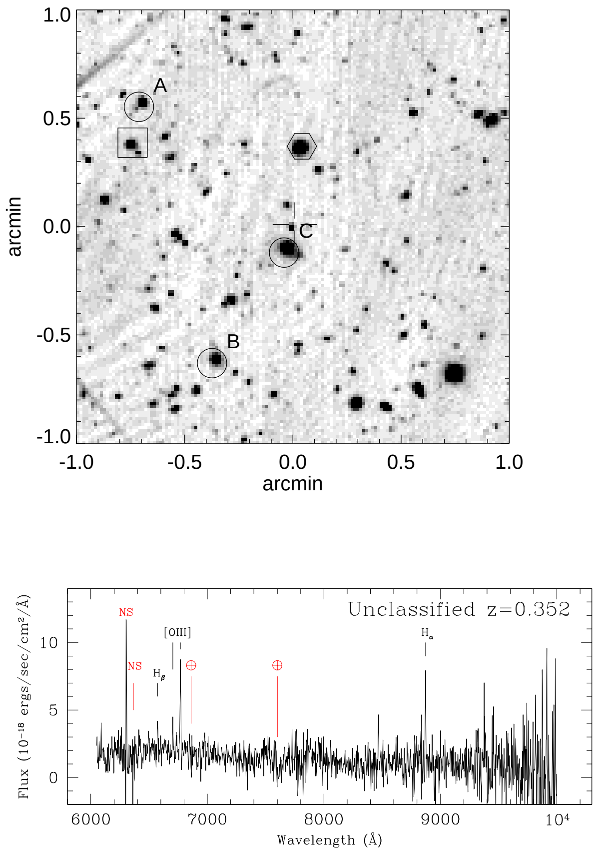

Fig. A.19. Above, a finding chart centered on SN 2002fp (C02-030), an unclassified candidate at $z = 0.352$, and below, the spectrum. The host galaxy has emission lines in [OIII] and H_β. The continuum is blue and, at this signal-to-noise ratio, featureless. This candidate might be a SN II, since the pre-maximum spectra of SNe II are generally featureless and blue; however, without clear features in the continuum, we cannot assign a classification.

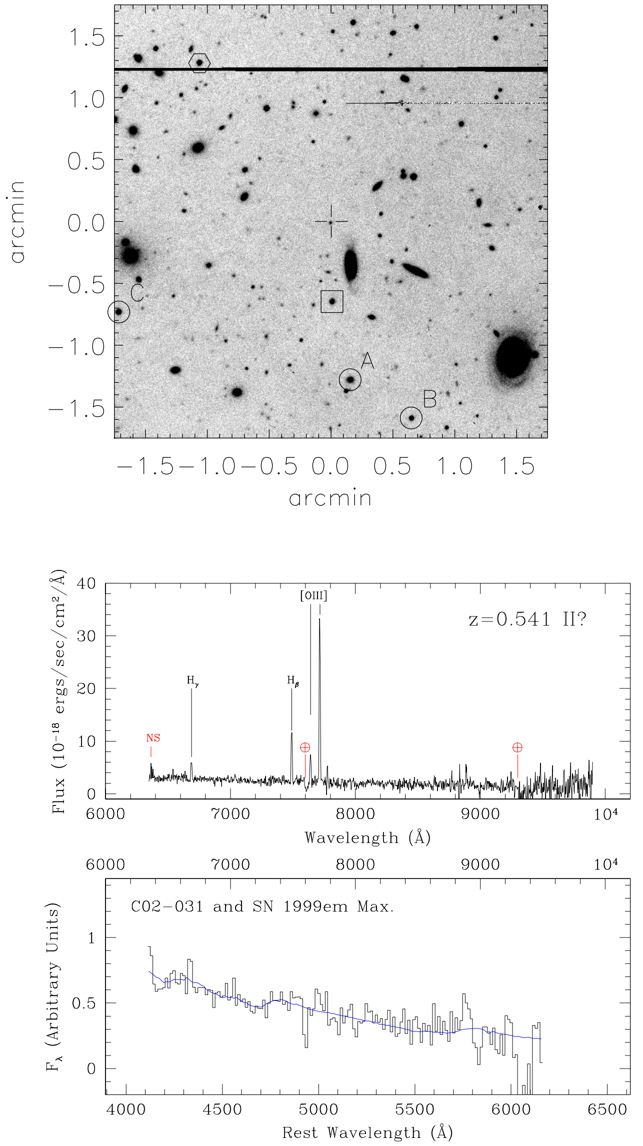

Fig. A.20. Above, a finding chart centered on C02-031, a possible Type II supernova at $z = 0.541$ and below, the spectrum. The host galaxy has emission lines in [OIII], H_β and H_γ. The tentative classification is based on the blue continuum and a weak H-beta line with a P-Cygni profile.

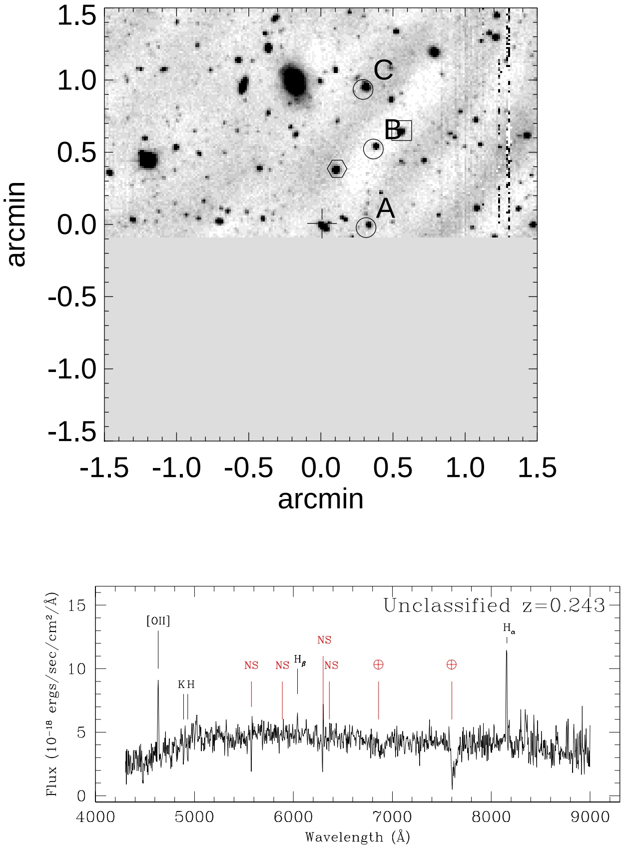

Fig. A.21. Above, a finding chart centered on C02-034, an unclassified candidate at $z = 0.243$, and below, the spectrum. The host galaxy has emission lines in H_α, H_β and [OII]. The Calcium H and K absorption lines are also visible.

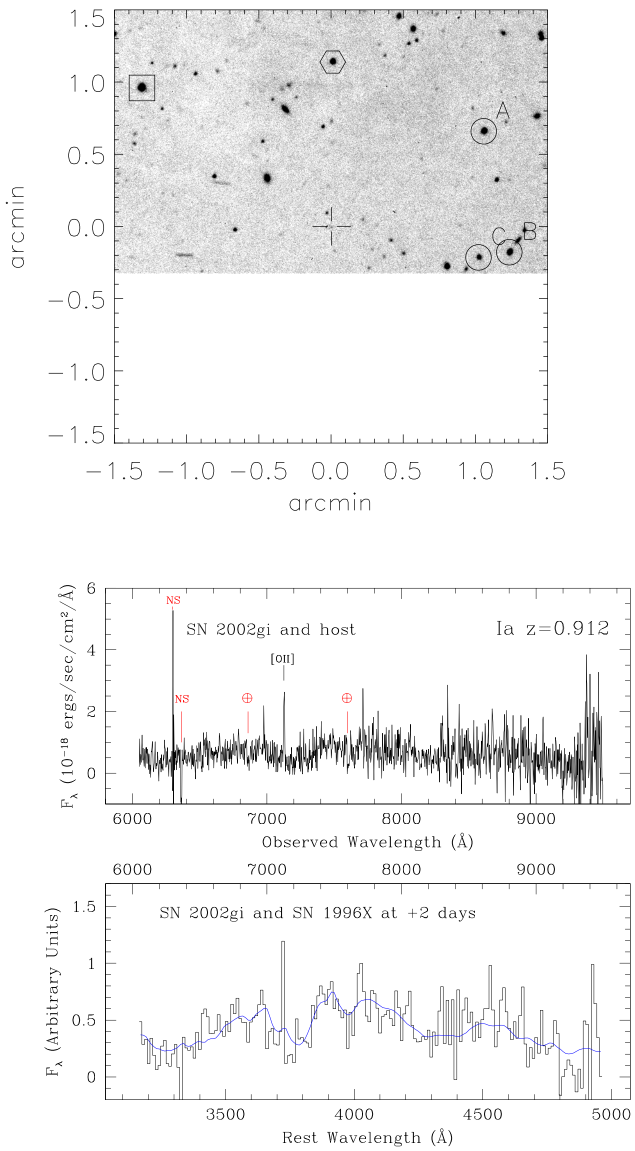

Fig. A.22. Above, a finding chart centered on SN 2002gi (T02-015), a SN Ia at z = 0.912, and below, the spectrum. The Si II 4000 Å feature is clearly detected in this high redshift candidate. This SN Ia has the highest redshift of all securely classified SNe Ia that were observed with FORS1.

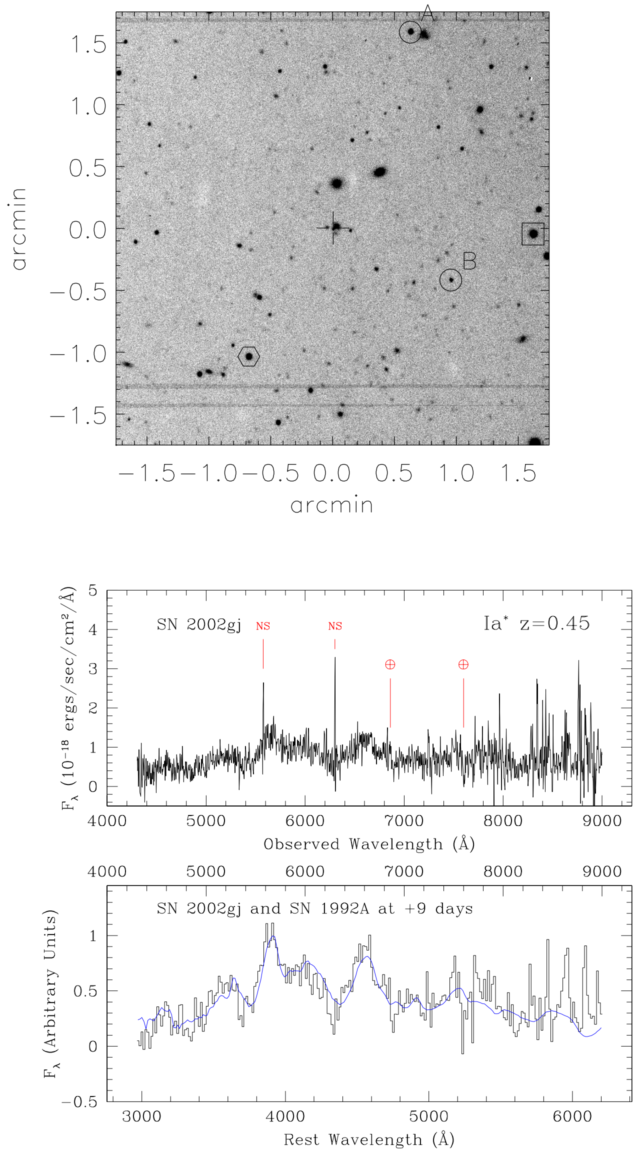

Fig. A.23. Above, a finding chart centered on SN 2002gj (T02-028), a SN Ia* at z = 0.45, and below, the spectrum. From the spectrum alone, this candidate can be matched with either a SN Ia at 10 days after maximum light or with a SN Ic near maximum light, so the classification is qualified with an asterisk. The time of maximum that is derived from the light curve shows that the spectrum was taken about 10 rest frame days after maximum light, so the the candidate is very likely to be a SN Ia.

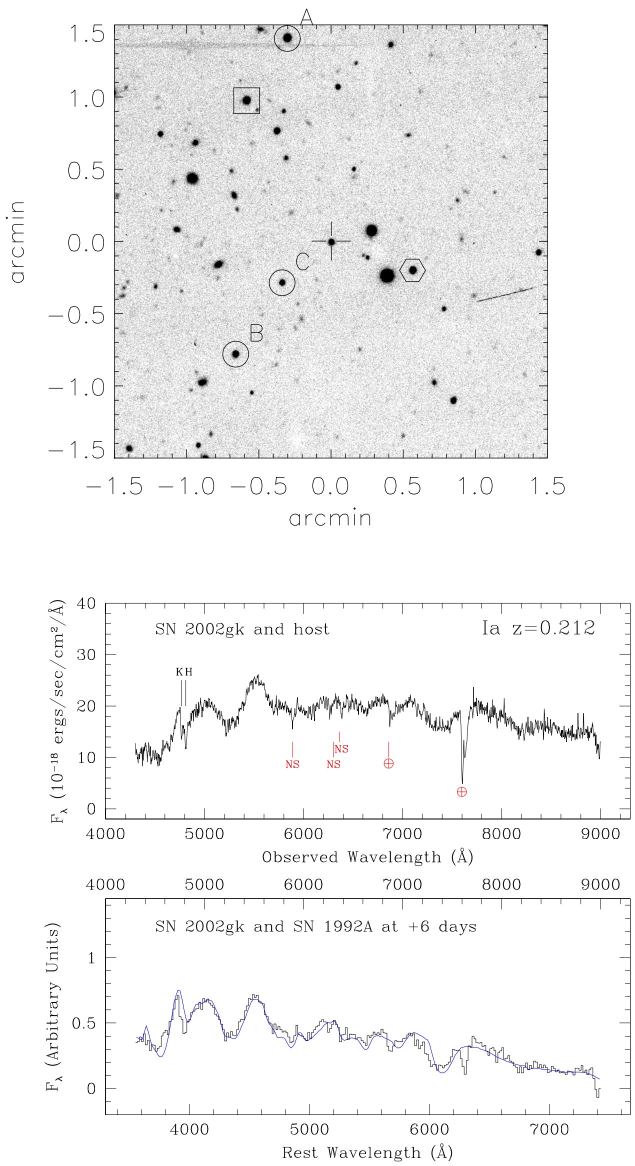

Fig. A.24. Above, a finding chart centered on SN 2002gk (T02-029), a SN Ia at z = 0.212, and below, the spectrum. This SN Ia has the lowest redshift and the spectrum has the highest signal-to-noise ratio of all candidates. Si II at 4000 Å and 6150 Å and S II at 5400 Å are all clearly detected.

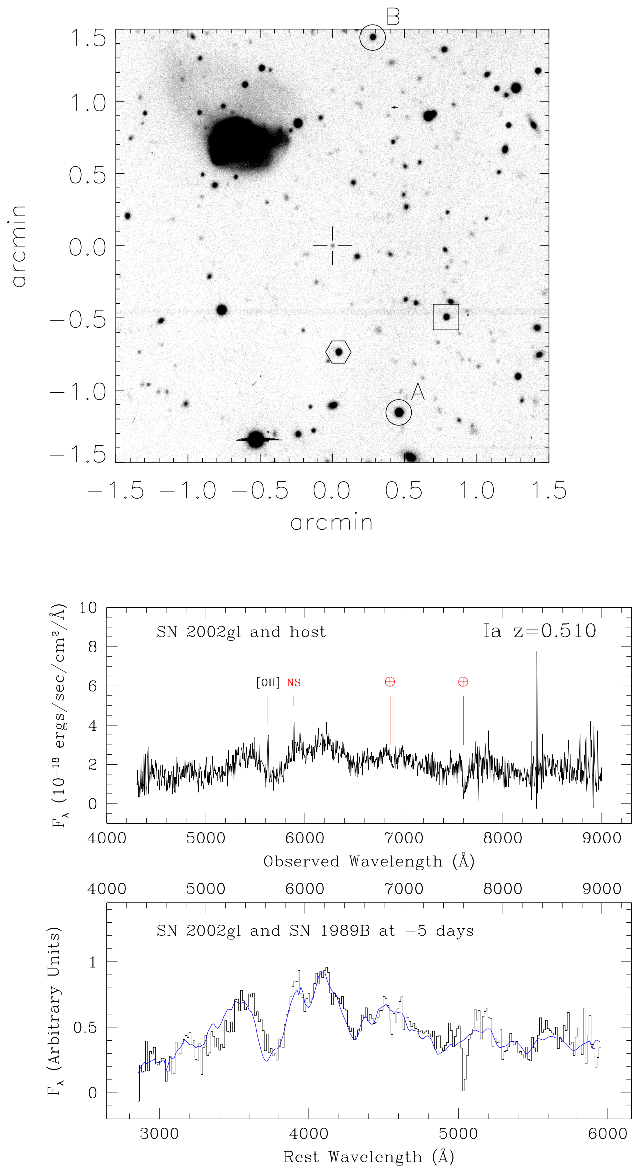

Fig. A.25. Above, a finding chart centered on SN 2002gl (T02-030), a SN Ia at z = 0.510, and below, the spectrum. Si II at 4000 Å and S II at 5400 Å are clearly detected in this candidate.

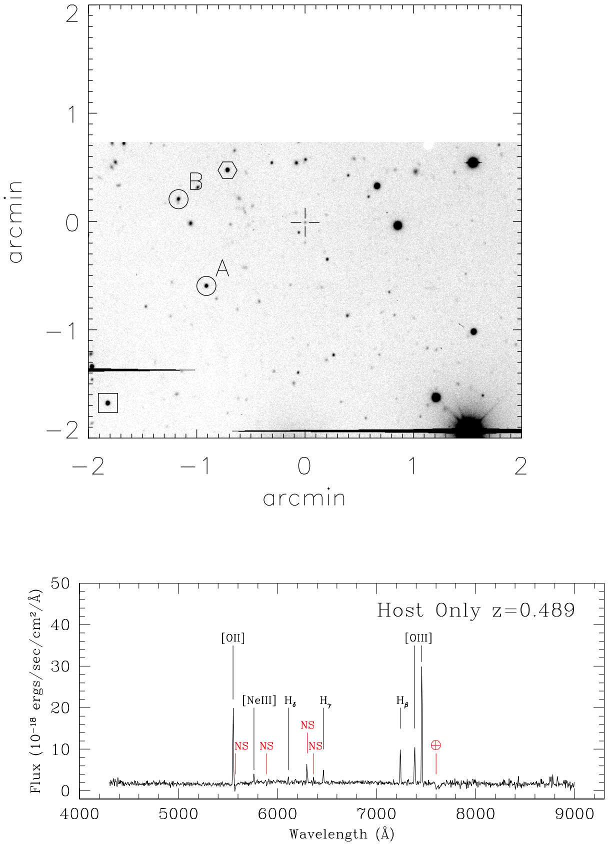

Fig. A.26. Above, a finding chart centered on T02-047, a probable supernova at $z = 0.489$, and below, the spectrum. The spectrum of the host was taken a couple of months after the candidate had faded and is rich in emission lines. Although a spectrum of the candidate was not obtained, the well-sampled light curve indicates that it is probably a supernova.

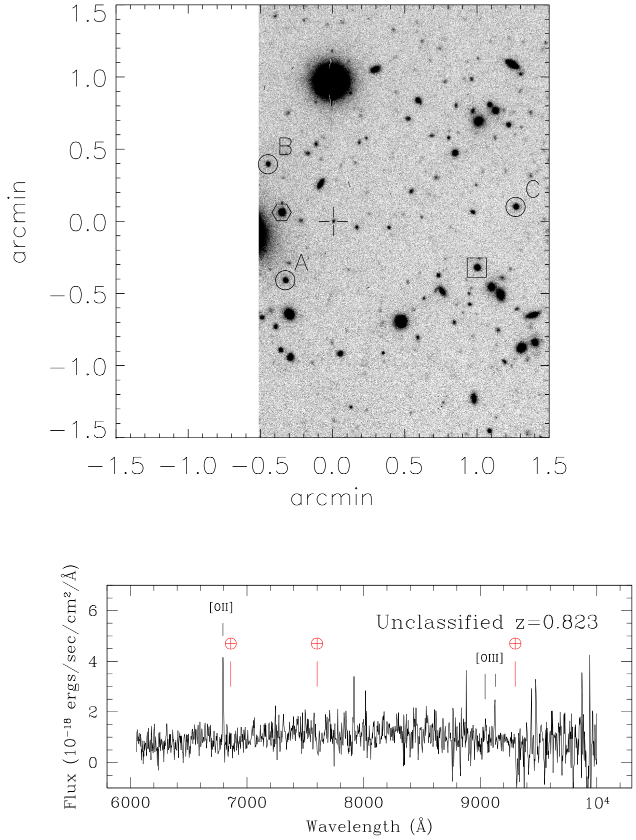

Fig. A.27. Above, a finding chart centered on SN 2002kq (SuF02-002), an unclassified candidate at $z = 0.823$, and below, the spectrum. This candidate was photometrically monitored and it has a supernova-like light curve.

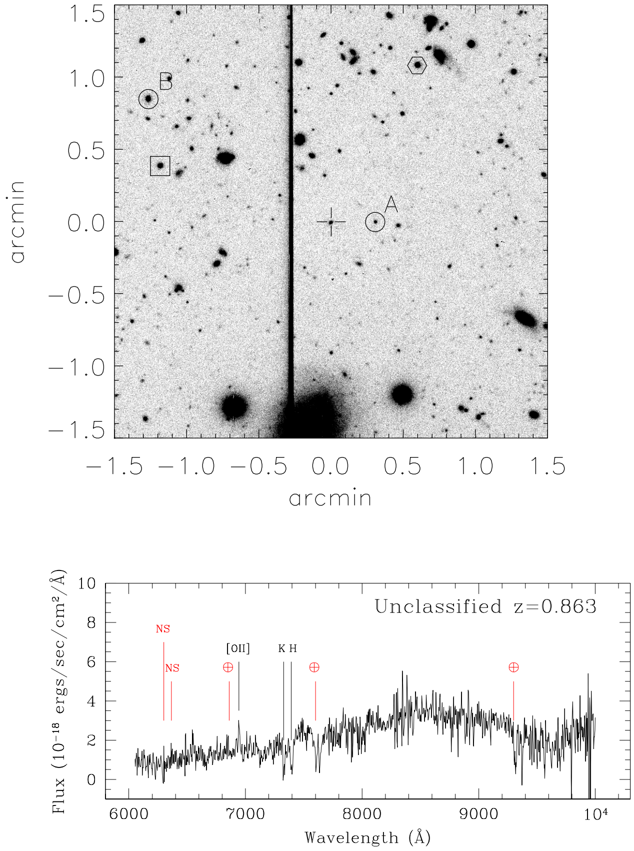

Fig. A.28. Above, a finding chart centered on SuF02-005, an unclassified candidate at z = 0.863, and below, the spectrum. This candidate has an extremely broad bump at 8500 Å. Since we observed the pivot star (object "A" in the finding chart) simultaneously with the candidate, we can use the flux-calibrated spectrum of the pivot star to check the calibration procedure. The flux-calibrated spectrum of star A does not have the broad feature that can be seen in the candidate, so the broad feature at 8500 Å is real.

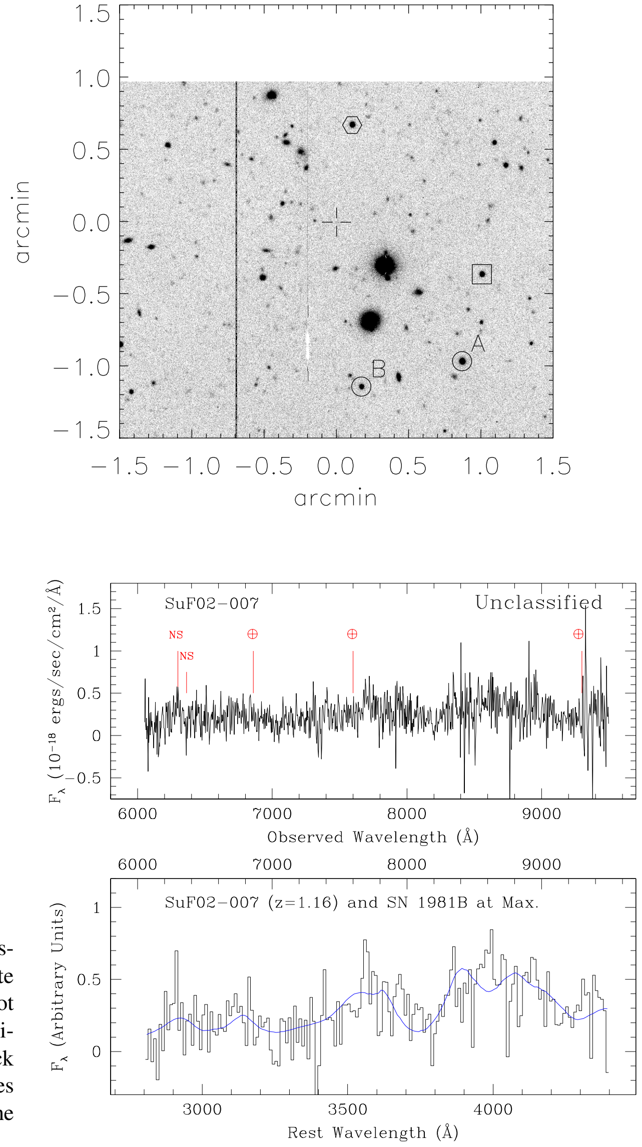

Fig. A.29. Above, a finding chart centered on SuF02-007 and below, the spectrum. The binned spectrum shows broad features that are consistent with a SN Ia at z = 1.16; however, the signal-to-noise ratio is too low for this candidate to be classified as a SN Ia from the spectrum alone. This candidate was photometrically monitored and has a supernova-like light curve.

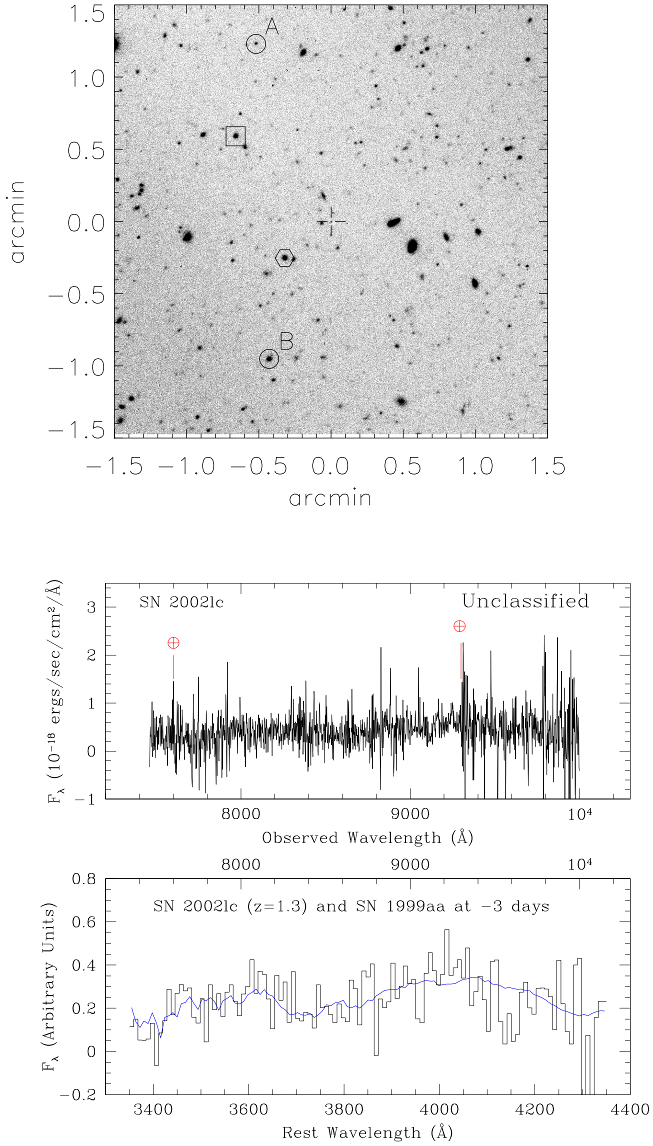

Fig. A.30. Above, a finding chart centered on SN 2002lc (SuF02-012) and below, the spectrum. The binned spectrum shows broad SN Ia like features which are consistent with a SN Ia at z = 1.3, however the signal-to-noise ratio is too small for a spectral classification. Hence, from the VLT spectrum alone it cannot be classified. However, SN 2002lc was also observed with FOCAS on Subaru, and the spectrum also shows similar broad features (Yasuda et al. in preparation). When added with the VLT data, a possible match with a SN Ia at z = 1.26 emerges. Furthermore, a spectrum of SN 2002lc was also taken with the ACS grism on HST. The reduced ACS spectrum shows the same broad features as the ground-based data. This candidate was photometrically monitored and has a supernova-like light curve.

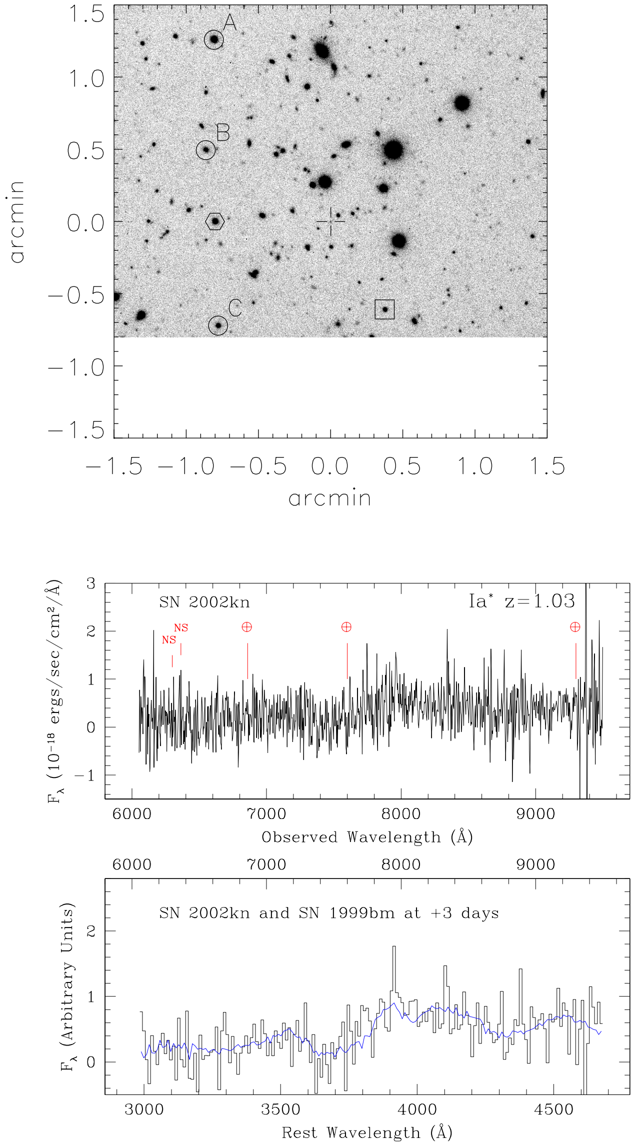

Fig. A.31. Above, a finding chart centered on SN 2002kn (SuF02-017), a SN Ia* at z=1.03, and below, the spectrum. The host galaxy is approximately three magnitudes fainter than the candidate, so the fraction of host galaxy light is set to zero in the fit. Since the Si II feature at 4000 Å is not clearly detected in this candidate and since there are no spectral features from the host, the redshift and the classification are derived from the fit. The spectrum can be fit equally well with a SN Ic, so the classification is qualified with an asterisk.

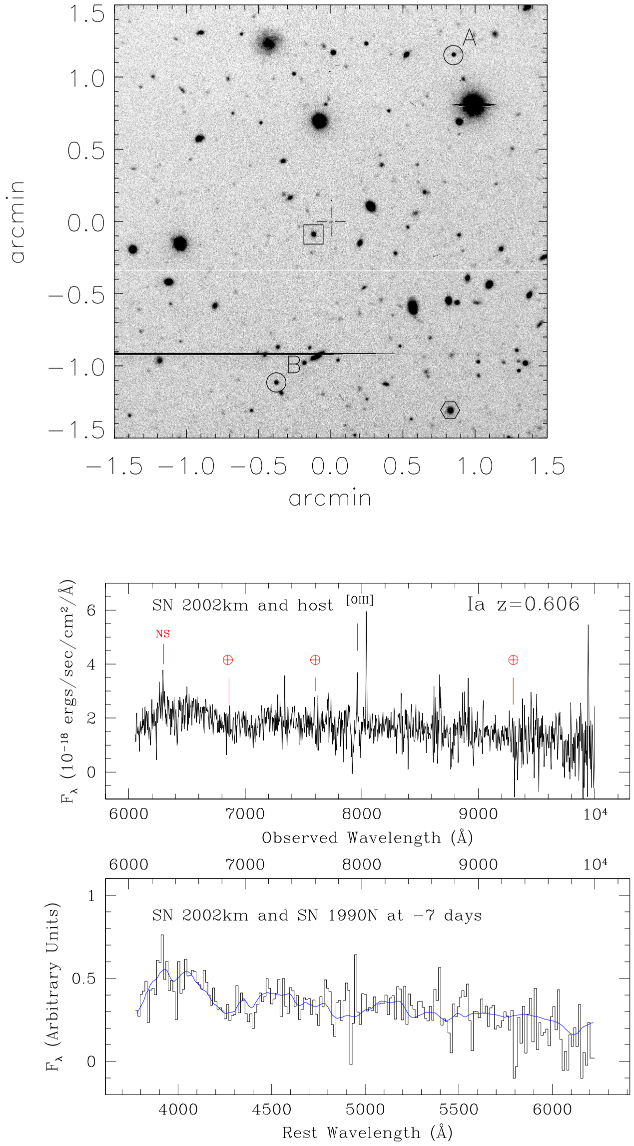

Fig. A.32. Above, a finding chart centered on SN 2002km (SuF02-025), a SN Ia at z = 0.606, and below, the spectrum. The Si II line at 4000 Å is clearly detected. There is a hint of the Si II line at 6150 Å.

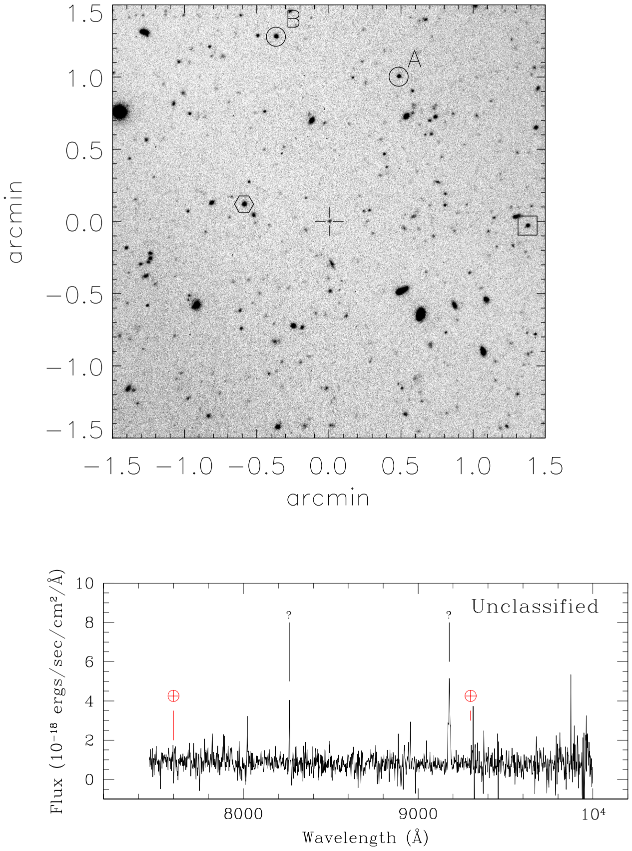

Fig. A.33. Above, a finding chart centered on SuF02-026 and below, the spectrum. This candidate has two unidentified emission lines with differing line profiles and spatial morphologies. The line at ~ 8300 Å is unresolved while the line at ~ 9200 Å is spatially and kinematically resolved into three components. This candidate was photometrically monitored and it has a supernova-like light curve.

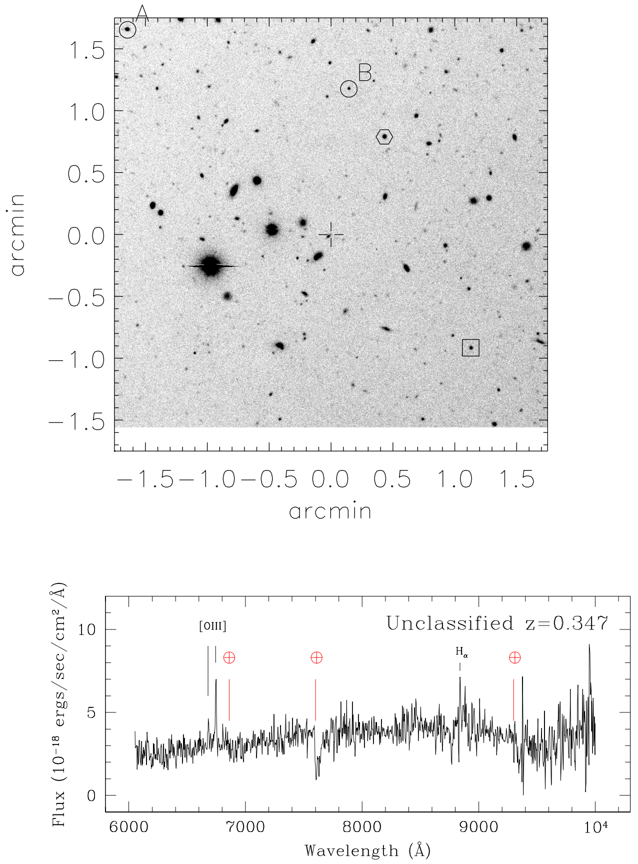

Fig. A.34. Above, a finding chart centered on SN 2002kn (SuF02-028), an unclassified candidate at $z = 0.347$, and below, the spectrum. This candidate is dominated by host galaxy light. It was photometrically monitored and it has a supernova-like light curve.

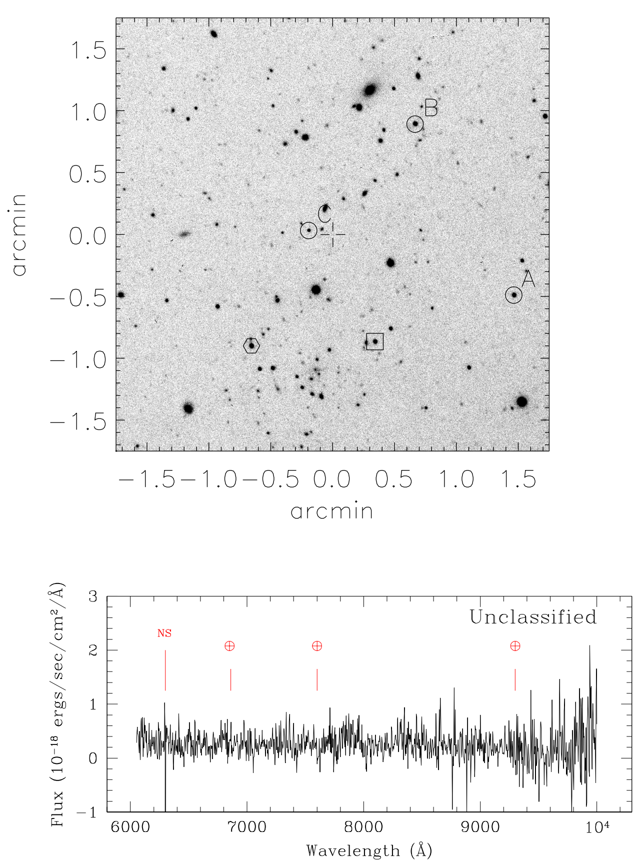

Fig. A.35. Above, a finding chart centered on SuF02-051, an unclassified candidate at an unknown redshift, and below, the spectrum. The spectrum is a featureless, slightly blue continuum. This candidate was photometrically monitored and it has a supernova-like light curve.

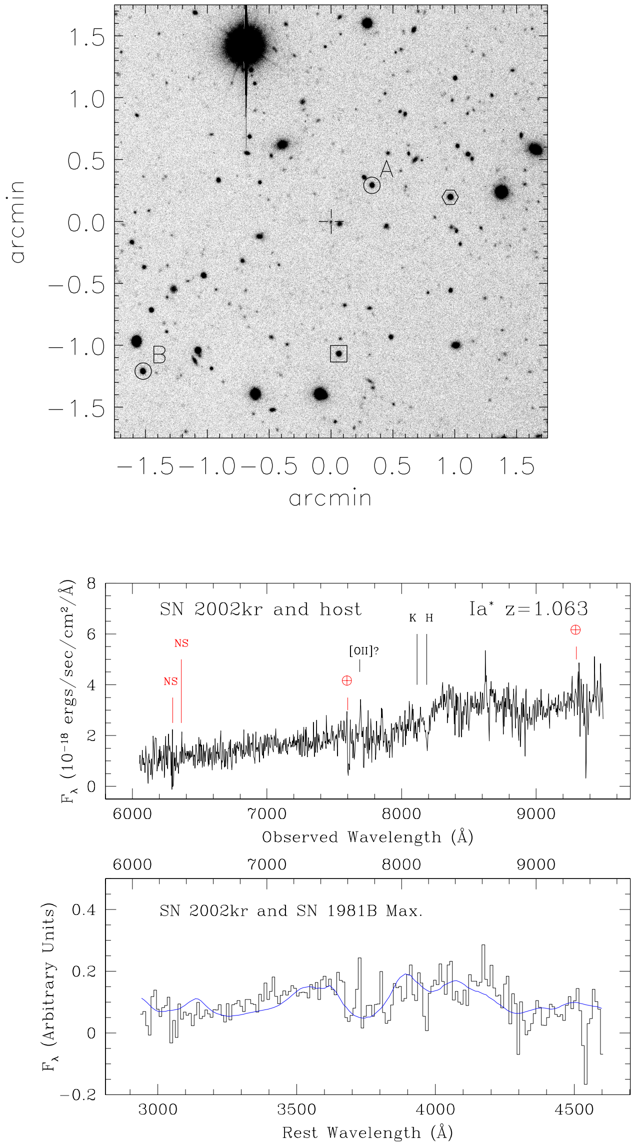

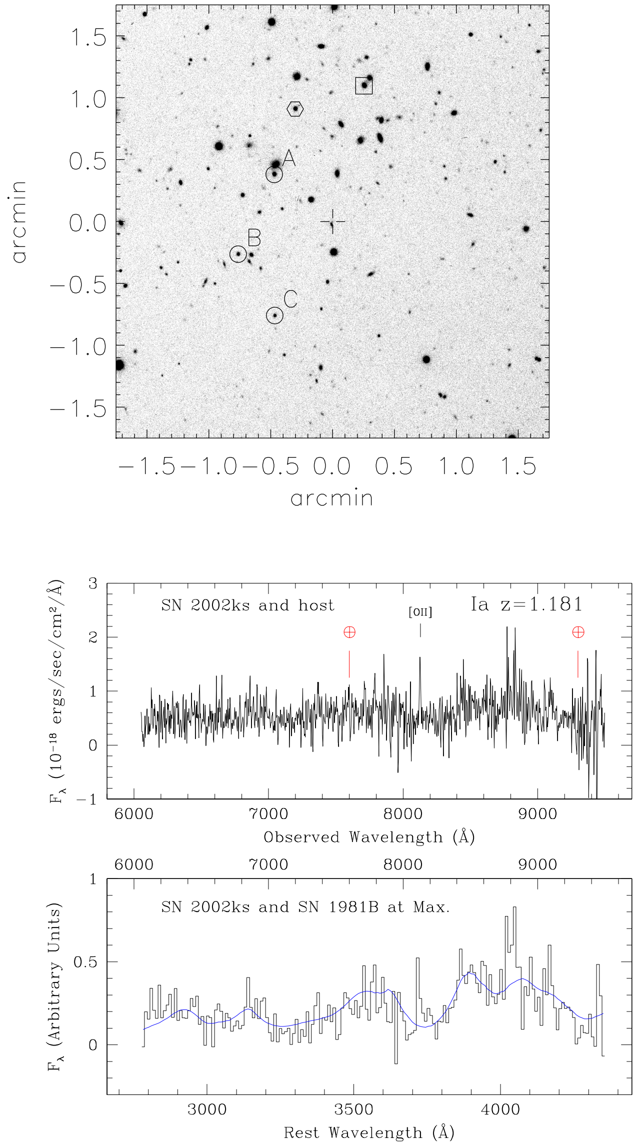

Fig. A.36. Above, a finding chart centered on SN 2002kr (SuF02-060), a SN Ia* at $z = 1.063$, and below, the spectrum. The redshift is determined from H and K Ca II absorption lines in the host. There is a hint of [OII] emission, but this is uncertain as the [OII] line at this redshift lies very close to atmospheric A band. The percentage increase was only 25%, so the spectrum is dominated by the host, which means that the host subtracted spectrum is sensitive to the host spectrum used in the fit. Hence, the classification is qualified with an asterisk. SN 2002kr was also observed with the ACS grism on HST and the GMOS spectrograph on Gemini. Both the Gemini and ACS show the same broad features as the VLT data.

Fig. A.37. Above, a finding chart centered on SN 2002ks (SuF02-065), a SN Ia at $z = 1.181$, and below, the spectrum. The Si II feature at 4000 Å is clearly detected. This SN Ia has the highest redshift of all securely classified SNe Ia that were observed with the ESO VLT.

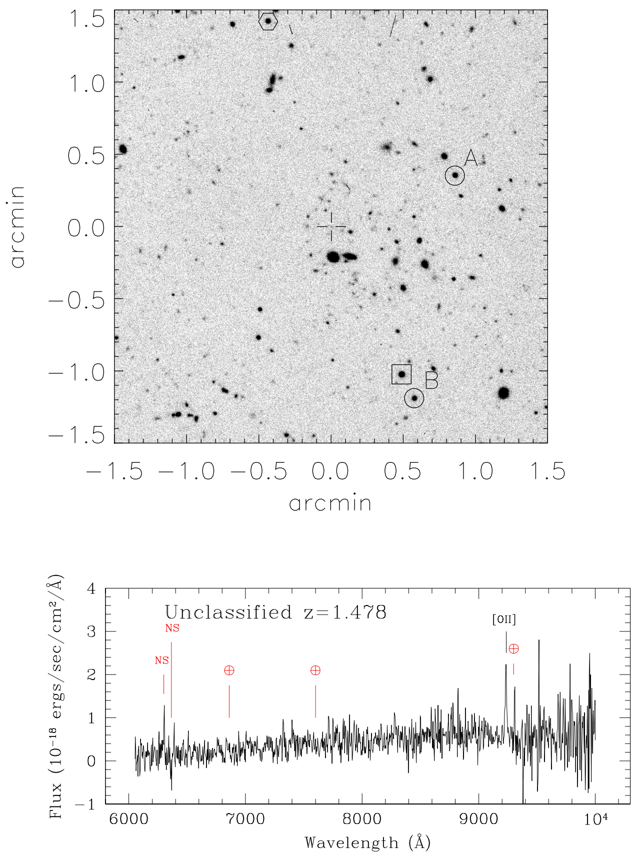

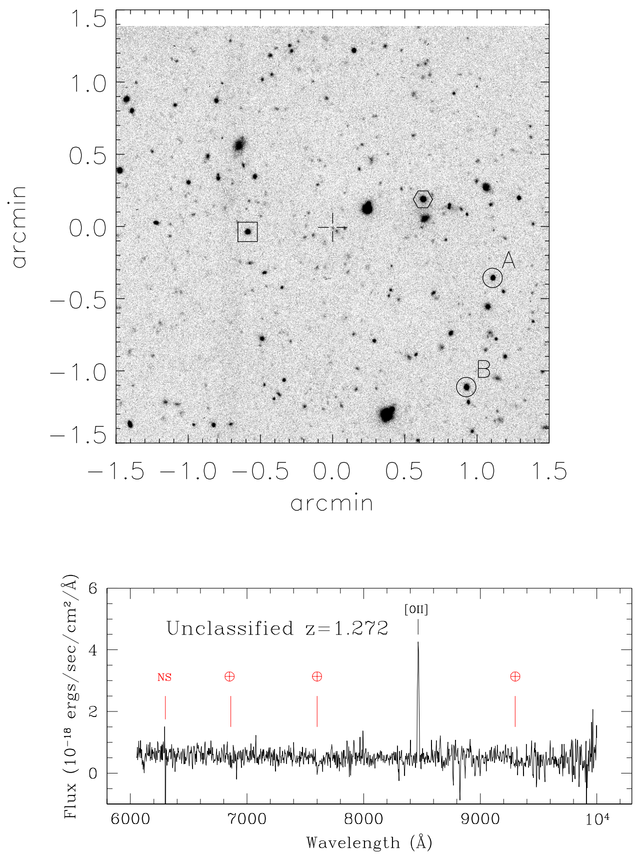

Fig. A.38. Above, a finding chart centered on SuF02-081, an unclassified candidate at z = 1.478 and below, the spectrum. A single strong line and a featureless red continuum. Like S02-001 and SN 2003kx we identify this line as the [OII] doublet at 3727 Å. This candidate was photometrically monitored and it has a light curve that is too narrow for it to be a SN Ia.

Fig. A.39. Above, a finding chart centered on SN 2003kx (SuF02-083), an unclassified candidate at z = 1.272, and below, the spectrum. A single strong line and a featureless continuum. Like S02-001 and SuF02-083, we identify this line as the [OII] doublet at 3727 Å.This candidate was photometrically monitored and it has a supernova-like light curve.